

JPL PUBLICATION 79-2

(NASA-CR-158,17) A GENERALIZED MODAL SHOCK
SPECTRA METHOD FOR SPACECRAFT LOADS ANALYSIS
(Jet Propulsion Lab.) 80 F HC A05/MF A01

N79-20177

CSCCL 22B

Unclas

G3/18 17264

A. Generalized Modal Shock Spectra Method for Spacecraft Loads Analysis

M. Trubert
M. Salama

March 15, 1979

National Aeronautics and
Space Administration

Jet Propulsion Laboratory
California Institute of Technology
Pasadena, California



JPL PUBLICATION 79-2

A Generalized Modal Shock Spectra Method for Spacecraft Loads Analysis

**M. Trubert
M. Salama**

March 15, 1979

National Aeronautics and
Space Administration

Jet Propulsion Laboratory
California Institute of Technology
Pasadena, California

The research described in this publication was carried out by the
Jet Propulsion Laboratory, California Institute of Technology, under
NASA Contract No. NAS7-100.

ACKNOWLEDGEMENT

The present work is a generalization of the original work, published and unpublished, pioneered by Robert H. Bamford of the Applied Mechanics Technology Section of JPL. Full acknowledgement is given to him for generating the fundamental ideas of making use of the shock spectra concept to determine bounds of loads in a spacecraft structure in the boost configuration. The effort was supported by the Office of Aeronautics and Space Technology.

ABSTRACT

Unlike an earlier shock spectra approach, the generalization presented in this paper permits an accurate elastic interaction between the spacecraft and launch vehicle to obtain accurate bounds on the spacecraft response and structural loads. In addition, the modal response from a previous launch vehicle transient analysis - with or without a dummy spacecraft - is exploited to define a modal impulse as a simple idealization of the actual forcing function. The idealized modal forcing function is then used to derive explicit expressions for an estimate of the bound on the spacecraft structural response and forces.

Greater accuracy is achieved with the present method over the earlier shock spectra, while saving much computational effort over the transient analysis.

ORIGINAL PAGE IS
OF POOR QUALITY

CONTENTS

I.	OVERVIEW -----	1-1
	A. BACKGROUND -----	1-1
	1. Transient Analysis -----	1-1
	2. Alternates to Transient Analysis -----	1-1
	3. Reduced Transient Analysis Method -----	1-2
	4. Shock Spectra Method -----	1-2
	5. The Generalized Shock Spectra Method -----	1-4
	B. OUTLINE OF THE GENERALIZED SHOCK SPECTRA -----	1-4
	C. BASIC ASSUMPTIONS -----	1-11
II.	BASIC EQUATIONS -----	2-1
III.	GENERALIZED MODAL DISPLACEMENT SPECTRA -----	3-1
	A. IDEALIZED EQUATIONS -----	3-1
	B. MODAL DISPLACEMENT SPECTRA -----	3-4
	C. DETERMINATION OF THE INITIAL MODAL VELOCITY v_{0l} -----	3-11
	1. Estimate of v_{0l} From the Modal Response -----	3-13
	2. Estimate of v_{0l} From Physical Interface Response -----	3-16
	D. TUNING -----	3-19
IV.	SPACECRAFT MEMBER LOADS, DISPLACEMENTS, AND ACCELERATION -----	4-1
	A. MEMBER LOADS -----	4-1
	B. DISPLACEMENTS AND ACCELERATIONS -----	4-3
	C. FLOW DIAGRAM -----	4-5
V.	CONCLUSIONS -----	5-1

CONTENTS (Continued)

REFERENCES ----- 5-2

APPENDIXES

A. ANALOG SOLUTION OF THE EQUATIONS OF MOTION ----- A-1

B. ANALYTICAL SOLUTION OF THE EQUATIONS OF MOTION ----- B-1

C. RECOVERY OF LAUNCH VEHICLE MODAL PROPERTIES ----- C-1

D. DISPLACEMENT SPECTRA FOR THE GENERALIZED RIGID BODY MODES ----- D-1

Figures

1-1. Shock Spectrum $S(\omega, \xi)$ of a Function $\ddot{x}_0(t)$ ----- 1-3

1-2. Composite System of Spacecraft and Launch Vehicle ---- 1-5

1-3. Idealization of Forcing Function ----- 1-8

3-1. Graphic Representation of $D_1(t)$, $D_2(t)$, and Their Approximate Maxima D_{1max} and D_{2max} ----- 3-9

3-2. Modal Displacement Spectra D_l and Q_l for a Launch Vehicle Mode l ----- 3-14

3-3. Shock Spectra Matching and Envelope ----- 3-18

4-1. Generalized Shock Spectra Method ----- 4-6

A-1. Launch Vehicle - Spacecraft Modal Model ----- A-6

A-2. Analog Schematic for Initial Velocity Solution ----- A-7

A-3. Analog Schematic for Impulse Solution ----- A-8

A-4. Mass Number 2 Response to Unit Impulse ----- A-9

A-5. Generalized Shock Spectra ----- A-10

A-6. Reduction Coefficient C ----- A-11

C-1. Composite Launch Vehicle With Elastically Loaded Interface ----- C-3

Table

A-1. Peak Acceleration ----- A-12

SECTION I

OVERVIEW

**ORIGINAL PAGE IS
OF POOR QUALITY**

A. BACKGROUND

1. Transient Analysis

The determination of the internal loads in a spacecraft structure subjected to a dynamic launch environment is an iterative process aimed at the ultimate sizing of the structure for its design. The process is iterative because the internal loads in the spacecraft are dependent upon the spacecraft mass and stiffness distribution, as well as the mass and stiffness distribution interaction with the launch vehicle. Some of the key parameters that dominate the loads analysis process are timeliness of the sizing, cost, weight limitations, and low sensitivity to iterative changes in the design. Because the loads are time-dependent functions, a complete transient analysis aimed at determining responses to given time-dependent forcing functions is widely used throughout the industry to determine loads in the launch vehicle and in the spacecraft. The transient analysis is a simulation method by which the loads time histories must be computed in their entirety before peak values can be identified for establishing design loads.

Although a transient analysis tends to result in lightweight designs when properly used, it is usually costly and time consuming, especially when several organizations are involved. No better method is presently known when dealing with a launch vehicle, and it is not suggested here that this process be changed for the launch vehicles. An alternate method is presented, however, for the analysis of the spacecraft.

2. Alternates to Transient Analysis

In the analysis of an aerospace structure, at least two organizations are involved: one organization responsible for the design and analysis of the launch vehicle, and another for the spacecraft. For the spacecraft-developing organization, it is desirable to perform frequent but inexpensive loads analyses to account for frequent design

changes in the spacecraft. Ideally, these analyses would include only the spacecraft, without requiring launch vehicle modeling and without requiring activity at the launch vehicle agency. For this reason, several alternatives have been suggested, and References 1-1 and 1-2 are recent examples. Like the method presented here, the methods given in References 1-1 and 1-2 apply only when the loads in the spacecraft result from time-dependent forcing functions applied on the launch vehicle, and bypass most of the costly time consuming steps of a complete transient solution.

3. Reduced Transient Analysis Method

The method of Reference 1-1 is a reduced transient analysis. Accelerations at the spacecraft-launch vehicle interface are obtained by a single transient analysis of the launch vehicle with a rigid mass. From this single launch vehicle analysis, interface accelerations can then be corrected to account for the elasticity of the spacecraft and used as input to the spacecraft. The correction procedure requires knowledge of the characteristics of the elastic spacecraft and of the rigid mass/elastic launch vehicle, but does not require the actual integration of the spacecraft elastic model with the launch vehicle elastic model, resulting in a significant cost reduction. From there on, the procedure follows the usual transient analysis.

4. Shock Spectra Method

Like the approach presented here, the method of Reference 1-2 is a generalization of the traditional shock spectra concept. In this concept, shown in Figure 1-1, a shock spectrum $S(\omega, \xi)$ of a function $\ddot{x}_0(t)$ is the largest peak response of a single-degree-of-freedom oscillator subjected to the base forcing function, $\ddot{x}_0(t)$. The implicit assumption is made that the input forcing function, $\ddot{x}_0(t)$, is not affected by the presence of the oscillator. This is true only if the mass of the oscillator is infinitesimal.

The most significant feature of Reference 1-2 was the introduction of the relative impedance between the spacecraft and the launch vehicle,

ORIGINAL PAGE IS
OF POOR QUALITY

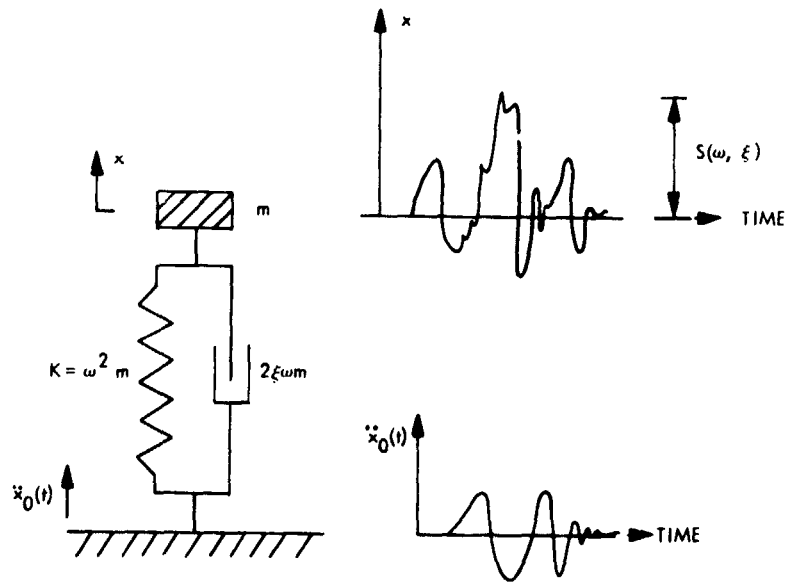


Figure 1-1. Shock Spectrum $S(\omega, \xi)$ of a Function $\ddot{x}_0(t)$

i.e., between the oscillator and the base, in the form of a reduction factor, C , which accounts for the effect of the oscillator on the interface acceleration. In addition, an envelope is constructed for the acceleration spectrum at the interface between the spacecraft and launch vehicle, Figure 1-2, which is used to determine the level of an equivalent sinusoidal forcing function to be applied at the interface for the computation of the spacecraft member loads. In this manner, spacecraft loads are computed with no integrated launch vehicle/spacecraft transient analysis. This method was applied to several spacecraft structures as reported in Reference 1-3, and was found to be much less costly to use, but produced somewhat heavier structures than a transient analysis.

In the application of the early shock spectra method outlined above, a number of assumptions were introduced that made its successful usage highly dependent upon the analyst's intuitive ability to recognize launch vehicle modes that are important to retain, and those of insignificant effects that can be discarded. The method sensitivity to the analyst's judgment is highlighted in the tacit assumption that the spacecraft/launch vehicle interface response is dominated almost totally by one launch vehicle mode at any one frequency, and in the process by which the envelope of the shock spectra is constructed.

5. The Generalized Shock Spectra Method

The present approach is an extension of Reference 1-2, with the objective of eliminating the analyst's judgment, formalizing the derivation and computational steps of the approach, explicitly stating the necessary assumptions, relaxing unessential ones, and introducing several significant improvements. These will be discussed in subsequent sections.

B. OUTLINE OF THE GENERALIZED SHOCK SPECTRA

The following general observations are fundamental to understanding the rationale of the shock spectra approaches:

- (1) The general objective is to avoid the cost of a launch vehicle/new spacecraft overall transient analysis.

ORIGINAL PAGE IS
OF POOR QUALITY

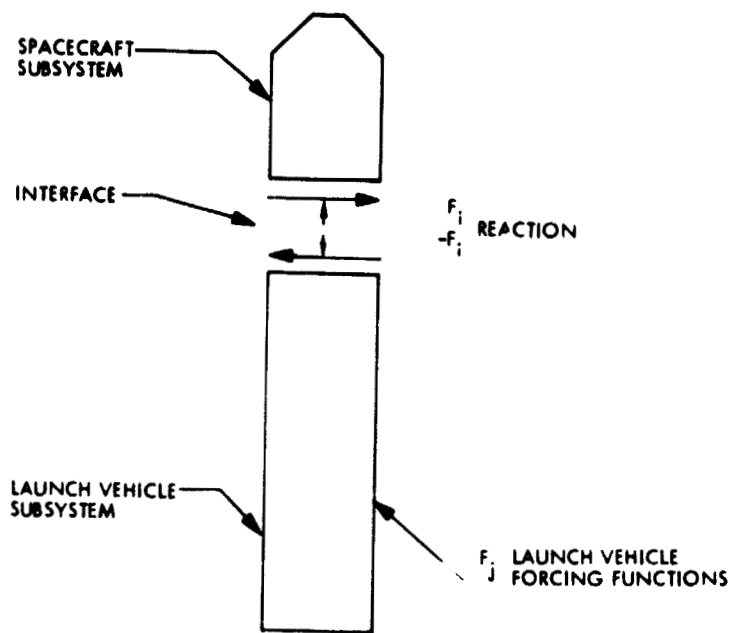


Figure 1-2. Composite System of Spacecraft and Launch Vehicle

- (2) There has been a previous dynamic analysis done for the launch vehicle with another or a dummy spacecraft, the results of which are used as inputs to the generalized shock spectra method. Note that the present method is derived for use of the modes of the launch vehicle loaded, by a rigid mass only, or not loaded. If such an analysis is not available, the proper data can still be recovered from the analysis of the launch vehicle loaded with an elastic spacecraft as shown in Appendix C.
- (3) The structural analyst needs only to determine the worst case load maxima or bounds, rather than time histories, of the structural response. Since maxima or bounds are the objective of the shock spectra concept, a shock spectra approach is readily applicable to the structural design process.
- (4) Any loads analysis - transient, shock spectra, or other - incorporates two basic items: a model idealizing the dynamic environment, i.e., the forcing function, and another idealizing the composite structural system. The form of each model is influenced by the selected approach, while its complexity is constrained by cost and time.
- (5) The original launch vehicle forcing functions, usually unknown to the spacecraft analyst, may be idealized by a simpler form to obtain an explicit closed form solution. A complete definition of this idealization is possible from the previous analysis of item (1) above, and is done at the modal level.

In view of these remarks, the generalized shock spectra method is highlighted as follows:

First, the modal forcing function $F_p(t)$ corresponding to the modes of the launch vehicle loaded by a rigid mass at the spacecraft interface, and representing the modal contribution of an actual flight

ORIGINAL PAGE IS
OF POOR QUALITY

event, is modeled, regardless of its physical point of application, by an equivalent launch vehicle modal forcing function, $F_{el}(t)$. Unlike the actual complex transient force, the equivalent forcing function chosen is a simpler form of variation with time. Here, an impulse delta function $F_{el}(t) = F_{Ol} \delta(t)$ with a yet-unknown magnitude F_{Ol} , or equivalently a velocity with magnitude v_{Ol} , is chosen for convenience.

The choice of a simplified forcing function as an impulse emphasizes the view that the shape of the response time history is of no consequence, and that only the peak or bound of the response is of interest. Therefore, any forcing function that would reproduce a response with the same maximum peak or bound as the actual forcing function is acceptable. The equivalency between the actual forcing function and the idealized one is established, not on the basis of producing identical response time histories, but on the basis of producing an identical peak of the shock spectra of each of the launch vehicle modal response $\ddot{q}_l(t)$, Figure 1-3, derived from the previously performed launch vehicle/dummy spacecraft analysis. An alternate to the direct use of $\ddot{q}_l(t)$ is discussed later.

The use of modal shock spectra, rather than the interface degrees-of-freedom shock spectra is significant because it automatically accounts for the matching of all interface physical degrees of freedom, and allows one to determine the modal magnitude of the impulse F_{Ol} or velocity v_{Ol} . It is noteworthy that the above process of establishing the equivalent idealized forcing function requires knowledge of the modal properties of the launch vehicle with or without a payload. Such information is usually available from the launch vehicle organization. Also note that the rigid mass at the launch vehicle/spacecraft interface does not have to be the total mass of the spacecraft to be analyzed, but can have any value convenient for the transient analysis performed earlier on the launch vehicle. The present approach does correct for whatever mass value was used.

Second, in considering the composite structural system of Figure 1-2, which consists of a spacecraft modeled by S-normal modes and a launch vehicle modeled by L-normal modes, there will be (S + L)

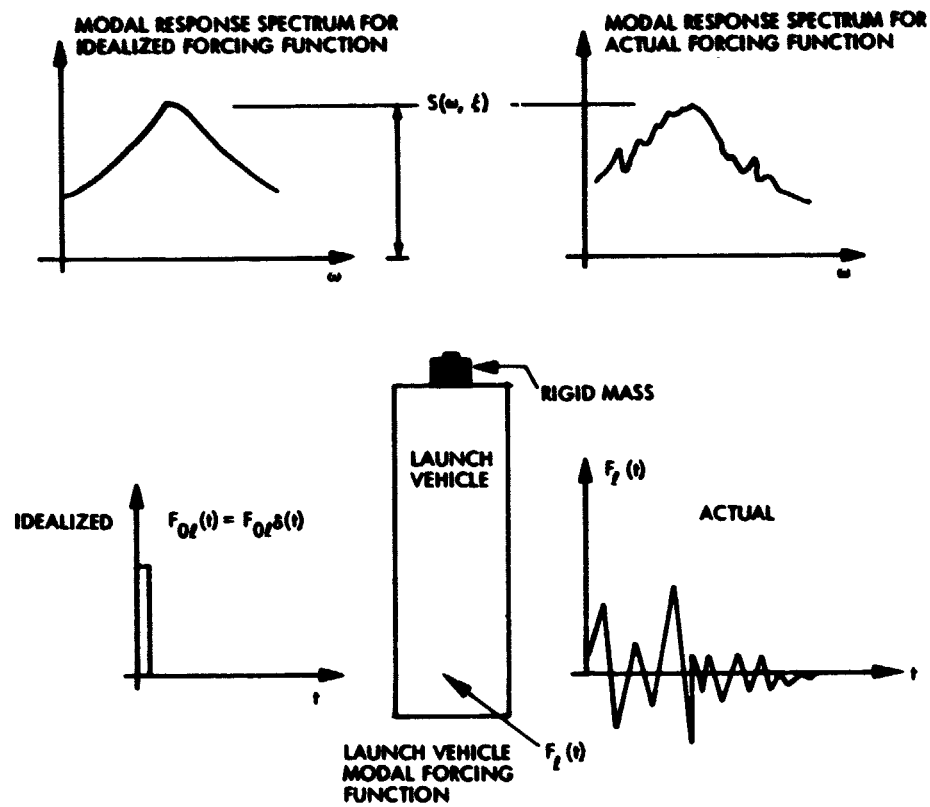


Figure 1-3. Idealization of Forcing Function

modally coupled equations of motion. Unlike the transient analysis where the solution is expressed in the complete $(S + L)$ space of modal coordinates and time, a bound on the complete solution is established herein by:

- (1) Idealizing the totality of $(S + L)$ mathematical space of modal coordinates by an array of nested $(S \times L)$ mathematical subspaces, in each of which only one spacecraft mode is individually coupled with one launch vehicle mode. In this fashion, each spacecraft mode is coupled with L -launch vehicle modes one at a time. To derive a bound on the total solution in the original $(S + L)$ mathematical space, an explicit solution in the form of spacecraft modal response time history is first derived for the pair of modes in a typical subspace. The explicit form of this solution is derived here, and is based on the idealized modal forcing function just discussed. Furthermore, because the spacecraft member loads are the objective of the analysis, and since these are proportional to the generalized modal displacements, the response quantities used here are generalized modal displacements, $q_{sl}(t)$, from which an expression of the bound Q_{sl} of $q_{sl}(t)$ is then derived.
- (2) Numerical computations are made first to establish the bounds, Q_{sl} , on each of the $(S \times L)$ discrete modal responses. Each bound Q_{sl} corresponds to one of the $(S \times L)$ subspaces. To account for unknown design tolerances and variations in the structural model idealization, worst cases can be provided by allowing realistic possible tuning between each spacecraft mode and its nearest launch vehicle mode, and by scaling the entire frequency spectrum of the launch vehicle with respect to that of the spacecraft.
- (3) Next, a bound on the total spacecraft modal response, Q_s , is constructed by summation over all the discrete L -bounds for that spacecraft mode. The summation can be over

absolute values, or in a root-sum-square sense that can also be weighted to account for phasing.

- (4) Finally, spacecraft member loads are obtained by adding the contributions of all spacecraft modes, either in absolute value or in a root-sum-square sense.

In the procedure outlined above, steps (1) and (2) derive expressions for bounds on the discrete response, Q_{sl} , in each of the $(S \times L)$ modal subspaces, while steps (3) and (4) construct a bound on the complete solution in the total $(S + L)$ space from the discrete Q_{sl} bounds. In this manner, much computational effort is saved over the usual transient analysis.

The significant improvements or differences from Reference 1-2 are:

- (1) Idealization of the actual forcing function by an impulse permits a simple evaluation of the shock spectra peaks. Other forms of forcing function idealizations could also be dealt with in the least square sense.
- (2) The shock spectra matching is applied to the modal - rather than the physical - degrees of freedom. This gives greater flexibility and more generality in the application of the procedure.
- (3) The modal displacement spectra, Q_{sl} , is derived for an arbitrary pair of coupled modes, a launch vehicle mode and a spacecraft mode, regardless of the proximity of their associated natural frequencies. Thus, the a priori selection of a specific launch vehicle mode on the basis of its relative significance in pairing with a given spacecraft mode is not required.
- (4) The entire treatment is believed to lend itself more readily to an automated spacecraft loads analysis that is substantially less dependent upon the analyst's intuitive ability.

ORIGINAL PAGE IS
OF POOR QUALITY

C. BASIC ASSUMPTIONS

Other than the usual assumption of linearity of structural behavior for both the spacecraft and launch vehicle, the following assumptions are made here:

- (1) The mass (and inertia) ratio between the spacecraft and the launch vehicle is small, but not necessarily infinitesimal.
- (2) The interface between the spacecraft and the launch vehicle is assumed statically determinate.
- (3) No external forces are acting directly upon the spacecraft other than through the common launch vehicle/spacecraft-interface.
- (4) A transient analysis of the launch vehicle with or without a dummy spacecraft is available.

Assumptions 1 and 2 are not overly restrictive, and could be relaxed without much difficulty. Removing assumption 2 would require introducing more complex basic equations. Assumption 2 can also be dealt with by introducing a portion of the launch vehicle interface in the spacecraft model. Other lesser assumptions are also made, and will be stated in subsequent sections as they arise.

SECTION II

BASIC EQUATIONS

A derivation of the equations of motion of a damped linear structural system under the action of prescribed forces $\{F_j(t)\}$ and prescribed rigid body accelerations $\{\ddot{R}(t)\}$ can be found in the literature (Reference 2-1). For each normal mode $n = 1, 2, \dots, N$, the equations may be written in the following form:

$$M_{nn}(\ddot{q}_n + 2\xi_n \omega_n \dot{q}_n + \omega_n^2 q_n) = \langle \phi_{nj} \rangle \{F_j\} - \langle M_{nR} \rangle \{\ddot{R}\} \quad (1)$$

where,

\ddot{R} = prescribed rigid body base motion

q_n = generalized modal coordinates that are related to the physical degrees-of-freedom, $\{u\}$, by the normal modes, $\{\phi_n\}$, such that $\{u_j\} = [\phi_{jn}] \{q_n\}$

$\{\phi_n\}$ = normal mode shape associated with q_n ; it is designated by $\{\phi_{jn}\}$ when evaluated at the j^{th} physical degree-of-freedom

ξ_n = percent of critical modal damping for the n^{th} mode

ω_n = natural frequency of the system, associated with q_n , $\{\phi_n\}$, and ξ_n

$\langle M_{nR} \rangle$ = mass coupling between elastic and rigid body modes

M_{nn} = elements of the diagonal modal mass matrix whose normalization is subsequently chosen so that $M_{nn} = 1$ for all modes

$\{F_j\}$ = time variable vector of forces applied at an arbitrary location j due to an arbitrary event

Equation (1) can be applied to a spacecraft mounted on a launch vehicle through a statically determinate interface as shown in Figure 1-2. Using subscripts s, l, and i to designate quantities associated, respectively, with the spacecraft, the launch vehicle, and their common interface i, Equation (1) can be separately written for the spacecraft and the launch vehicle by taking proper account of the reaction forces, $\{F_i\}$, and accelerations, $\{\ddot{R}_i\}$, at the interface. The results are:

for the l^{th} normal mode of the free-free launch vehicle

$$\ddot{q}_l + 2\xi_l \omega_l \dot{q}_l + \omega_l^2 q_l = \langle \phi_{lj} \rangle \{F_j\} - \langle \phi_{li} \rangle \{F_i\} \quad (2)$$

or the s^{th} normal mode of the spacecraft, cantilevered from i,

$$\ddot{q}_s + 2\xi_s \omega_s \dot{q}_s + \omega_s^2 q_s = -\langle m_{si} \rangle \{\ddot{R}_i\} \quad (3)$$

In Equations (2) and (3), the interface acceleration, $\{\ddot{R}_i\}$, is obtained by superposition of the contributions of all launch vehicle modes, rigid and elastic:

$$\{\ddot{R}_i\} = [\phi_{iR}] \{\ddot{q}_R\} + [\phi_{i\ell}] \{\ddot{q}_\ell\} \quad (4)$$

The launch vehicle rigid body acceleration $\{\ddot{q}_R\}$ above is obtained as a special case of Equation (2) when $\omega_l = 0$:

$$[M_{RR}] \{\ddot{q}_R\} = [\phi_{Rj}] \{F_j\} - [\phi_{Ri}] \{F_i\} \quad (5)$$

Furthermore, the reaction forces, $\{F_i\}$, on the statically determinate spacecraft-to-launch vehicle interface are obtained by summing the reactions for all spacecraft modes T:

$$\{F_i\} = \left(\sum_{s=1}^T [m_{ii}^s] \{\ddot{R}_i\} \right) + [m_{is}] \{\ddot{q}_s\} \quad s = 1, 2, \dots, T \quad (6)$$

ORIGINAL PAGE IS
OF POOR QUALITY

in which $[m_{ii}^s]$ is the contribution of each mode s to the rigid mass matrix relative to the interface i . The following relationship holds for each mode s :

$$[m_{ii}^s] = [m_{is}] \langle m_{si} \rangle$$

Rather than including all spacecraft modes, only a truncated or selected set of modes $S < T$ are usually retained. Such truncation or selection may be done by including a residual rigid mass $[M_{ii}]_{RES}$ defined by (Reference 2-2):

$$[M_{ii}]_{RES} = [M_{ii}] - \sum_{s=1}^S [m_{ii}^s] \quad (7)$$

where $[M_{ii}]$ is the total rigid body mass matrix when all T modes are considered;

$$[M_{ii}] = [m_{is}] [m_{si}]$$

Therefore, Equation (6) for $\{F_i\}$, can in general, be replaced by:

$$\{F_i\} = [M_{ii}]_{RES} \{\ddot{R}_i\} + \left(\sum_{s=1}^S [m_{ii}^s] \right) \{\ddot{R}_i\} + [m_{is}] \{\ddot{q}_s\} \quad (8)$$

In Equation (8), the neglected modes are represented by their equivalent rigid mass, regardless whether their frequencies are higher or lower than the range in question. In this manner one is able to consider the elastic mass contributions of as few or as many spacecraft modes as desirable, with the remaining modes contributing to the residual rigid mass. A greater number of elastic modes result in a smaller residual rigid mass matrix, which approaches zero when all elastic modes have been included. From a modeling point of view, such

a residual mass matrix can also have a wide range of applications in representing the mass characteristics of part or all of the spacecraft during the various cycles of loads analysis. In particular, the residual mass term allows the analyst to use directly the modes of the launch vehicle loaded by a rigid mass.

For S-spacecraft and L-launch vehicle elastic modes, Equations (2) and (3), along with their companion expressions (4), (5), and (8) result in (S + L) coupled equations describing the motion of the composite spacecraft-launch vehicle system. Instead of the commonly used transient analysis for the solution of this system of equations, a generalization of the shock spectra concept will be developed next, with the aim of obtaining a bound on the solution rather than its detailed time history.

SECTION III

GENERALIZED MODAL DISPLACEMENT SPECTRA

A. IDEALIZED EQUATIONS

In a full transient analysis of the coupled (S + L) Equations (2) and (3), all modes are simultaneously considered, and the solution is sought as time histories of the response quantities of interest. Since bounds rather than time histories are needed for design, much computational effort can be saved by introducing mathematical idealizations that allow a relatively simple estimate of the bounds. This is achieved here when the entire (S + L) mathematical space of modal coordinates is idealized by an array of nested (S × L) mathematical discrete subspaces. In each subspace, a spacecraft mode s is coupled with a launch vehicle mode l, thus giving rise to (S × L) possible pairings. A bound on the true solution in the original (S + L) mathematical space is established by summation over the individual discrete bounds in the (S × L) subspaces.

Because the spacecraft member loads are the object of the analysis here, and since these are proportional to the generalized modal displacements q_s , bounds on the spacecraft member loads are expressed in terms of the bounds, Q_{sl} , of the generalized modal displacements for each subspace. A typical generalized modal displacement bound, Q_{sl} , is derived here for a typical subspace in which one spacecraft mode q_s is coupled with one launch vehicle mode q_l . For this purpose, Equations (4), (5), and (8) are solved together to yield:

$$\left. \begin{aligned} \{\ddot{R}_i\} &= \left([I] + [\psi_{ii}] [M_{ii}^S] \right)^{-1} \left([\psi_{ij}] \{F_j\} + \{\phi_{il}\} \ddot{q}_l - [\psi_{ii}] \{m_{is}\} \ddot{q}_s \right) \\ \{F_i\} &= \left([I] + [M_{ii}^S] [\psi_{ii}] \right)^{-1} \left([M_{ii}^S] [\psi_{ij}] \{F_j\} + [M_{ii}^S] \{\phi_{il}\} \ddot{q}_l + \{m_{is}\} \ddot{q}_s \right) \end{aligned} \right\} (9)$$

where

$$[M_{ii}^S] = [M_{ii}]_{RES} + [m_{ii}^S]$$

$$[\psi_{ii}] = [\phi_{iR}] [M_{RR}^{-1}] [\phi_{Ri}]$$

$$[\psi_{ij}] = [\phi_{iR}] [M_{RR}^{-1}] [\phi_{Rj}]$$

If the ratio of the Euclidian norm¹ of the rigid mass matrix, $[M_{ii}^S]$ defined above for the spacecraft, to the norm of the total rigid launch vehicle mass matrix, $[M_{RR}]$, is small, a simplifying approximation can be introduced in Equation (9), in which

$$[M_{ii}^S] [\psi_{ii}] = [M_{ii}^S] [\phi_{iR}] [M_{RR}^{-1}] [\phi_{Ri}] \doteq 0 \quad (10)$$

$$[M_{ii}^S] [\psi_{ij}] = [M_{ii}^S] [\phi_{iR}] [M_{RR}^{-1}] [\phi_{Rj}] \doteq 0$$

This results in the approximate set of equations for $\{\ddot{R}_i\}$ and $\{F_i\}$:

$$\{\ddot{R}_i\} = [\psi_{ij}] \{F_j\} + \{\phi_{i\ell}\} \ddot{q}_\ell - [\psi_{ii}] \{m_{is}\} \ddot{q}_s \quad (11)$$

$$\{F_i\} = [M_{ii}^S] \{\phi_{i\ell}\} \ddot{q}_\ell + \{m_{is}\} \ddot{q}_s$$

which, when substituted into Equations (2) and (3), yields the following simplified version of the equations of motion for an arbitrary pair of coupled spacecraft and launch vehicle modes:

¹As a measure of the magnitude of a matrix A, the Euclidian norm is defined in analogy with the length of a vector by

$$N(A) = \left(\sum_i \sum_j a_{ij}^2 \right)^{1/2}$$

where a_{ij} are the elements of A.

$$\begin{aligned}
 & \left[\begin{array}{c|c} 1 + \langle \phi_{li} \rangle [M_{ii}^S] \langle \phi_{il} \rangle & \langle \phi_{li} \rangle \langle m_{is} \rangle \\ \hline \langle m_{si} \rangle \langle \phi_{il} \rangle & 1 \end{array} \right] \begin{Bmatrix} \ddot{q}_l \\ \ddot{q}_s \end{Bmatrix} + \left[\begin{array}{c|c} 2\xi_l \omega_l & 0 \\ \hline 0 & 2\xi_s \omega_s \end{array} \right] \begin{Bmatrix} \dot{q}_l \\ \dot{q}_s \end{Bmatrix} \\
 & + \left[\begin{array}{c|c} \omega_l^2 & 0 \\ \hline 0 & \omega_s^2 \end{array} \right] \begin{Bmatrix} q_l \\ q_s \end{Bmatrix} = \begin{Bmatrix} \langle \phi_{lj} \rangle \langle F_j \rangle \\ 0 \end{Bmatrix} \quad (12)
 \end{aligned}$$

Note that removing the assumption that lead to Equation (10) will result only in redefining the terms of Equations (11) and (12). Also, although similar to Equation (C-5) of Appendix C, Equation (12) holds for only one launch vehicle mode and one spacecraft mode at a time, unlike Equation (C-5), which holds for all modes.

In Equation (12),

$$\begin{aligned}
 \langle \phi_{li} \rangle [M_{ii}^S] \langle \phi_{il} \rangle &= \langle \phi_{li} \rangle [M_{ii}]_{RES} \langle \phi_{il} \rangle + \langle \phi_{li} \rangle \langle m_{is} \rangle \langle m_{si} \rangle \langle \phi_{il} \rangle \\
 &= M_{sl} + m_{sl}
 \end{aligned}$$

where

$$M_{sl} = \langle \phi_{li} \rangle [M_{ii}]_{RES} \langle \phi_{il} \rangle = m_{sl} + \langle \phi_{li} \rangle [M_0] \langle \phi_{il} \rangle$$

$$m_{sl} = \langle \phi_{li} \rangle [m_{ii}^S] \langle \phi_{il} \rangle = \langle \phi_{li} \rangle \langle m_{is} \rangle \langle m_{si} \rangle \langle \phi_{il} \rangle$$

Then, Equation (12) can be rewritten in the following more convenient form:

$$\begin{aligned}
 & \left[\begin{array}{c|c} (1 + \mu_{sl}) & \mu_{sl} \\ \hline \mu_{sl} & \mu_{sl} \end{array} \right] \begin{Bmatrix} \ddot{x}_1 \\ \ddot{x}_2 \end{Bmatrix} + \left[\begin{array}{c|c} 2\xi_1 \omega_1 & 0 \\ \hline 0 & 2\xi_2 \omega_2 \mu_{sl} \end{array} \right] \begin{Bmatrix} \dot{x}_1 \\ \dot{x}_2 \end{Bmatrix} \\
 & + \left[\begin{array}{c|c} \omega_1^2 & 0 \\ \hline 0 & \omega_2^2 \mu_{sl} \end{array} \right] \begin{Bmatrix} x_1 \\ x_2 \end{Bmatrix} = \begin{Bmatrix} F_l(t) \\ 0 \end{Bmatrix} \quad (13)
 \end{aligned}$$

in which the following additional definitions have been used:

$$\mu_{sl} = \frac{m_{sl}}{1 + M_{sl}}$$

$$\omega_1 = \frac{\omega_l}{\sqrt{1 + M_{sl}}}$$

$$\xi_1 = \frac{\xi_l}{\sqrt{1 + M_{sl}}}$$

$$\omega_2 = \omega_s$$

$$\xi_2 = \xi_s$$

$$F_l(t) = \langle \phi_{lj} \rangle \{F_j(t)\}$$

$$q_l = \left(\frac{1}{1 + M_{sl}} \right) x_1$$

$$q_s = \left(\frac{\langle m_{sl} \rangle \{ \phi_{1l} \}}{1 + M_{sl}} \right) x_2 = \left(\frac{\pm \sqrt{m_{sl}}}{1 + M_{sl}} \right) x_2$$

(14)

B. MODAL DISPLACEMENT SPECTRA

The pair of modally coupled equations in Equation (13) describe the motion in any of the idealized ($S \times L$) subspaces where a spacecraft mode is coupled with a launch vehicle mode. A bound on the spacecraft generalized modal displacement in such subspace is derived in this section from an explicit time-dependent solution of Equation (13), in which the actual launch vehicle modal forcing function $F_l(t)$ is modeled

by an equivalent forcing function having a simpler form of variation with time. The selected idealization of the forcing function is an impulse delta function having a magnitude $F_{0\ell}$, or alternatively, an initial velocity with a magnitude $v_{0\ell}$.

The equivalency between the actual forcing function and the idealized one is established on the basis of producing identical bounds on the modal displacement. This requirement yields one equation for the definition of the magnitude of the initial impulse or velocity. The choice of an initial impulse or velocity as an idealization of the actual forcing function is made here only for simplicity of the resulting solution. In fact, any other choice of time variation for the idealized forcing function is acceptable, provided that the above mentioned equivalency condition is enforced. For example, a sinusoidal idealization (as in Reference 1-2) in terms of two unknown parameters, a magnitude and a frequency, could be used. By enforcing more than two condition equations, one could determine the two unknowns, magnitude and frequency, in the least square sense. Functions of higher number of known parameters could be dealt with in a similar fashion.

An analog computer solution of Equation (13) is given in Appendix A for a modal delta function impulse of magnitude $F_{0\ell}$, associated with a launch vehicle mode ℓ . Also, details of the analytical solution to the same equations are given in Appendix B for the equivalent modal initial velocity $v_{0\ell}$. The analytical expressions for $x_1(t)$ and $x_2(t)$ are written as:

$$\begin{aligned}
 x_1(t) &= \frac{v_{0l}}{(\Omega_2^2 - \Omega_1^2)} \left[\frac{\Omega_2^2(1 - \Omega_1^2)}{\bar{\omega}_{n1}} e^{-\xi_{n1}\omega_{n1}t} \sin \bar{\omega}_{n1}t \right. \\
 &\quad \left. - \frac{\Omega_1^2(1 - \Omega_2^2)}{\bar{\omega}_{n2}} e^{-\xi_{n2}\omega_{n2}t} \sin \bar{\omega}_{n2}t \right] \\
 x_2(t) &= \frac{R^2 v_{0l}}{(\Omega_2^2 - \Omega_1^2)} \left[\frac{1}{\bar{\omega}_{n1}} e^{-\xi_{n1}\omega_{n1}t} \sin \bar{\omega}_{n1}t \right. \\
 &\quad \left. - \frac{1}{\bar{\omega}_{n2}} e^{-\xi_{n2}\omega_{n2}t} \sin \bar{\omega}_{n2}t \right]
 \end{aligned} \tag{15}$$

The following parameters have been used in Equation (15):

$$\begin{aligned}
 \omega_{n1} &= \omega_2 \Omega_1, & \omega_{n2} &= \omega_2 \Omega_2 \\
 \Omega_1 &= \Omega_0 - \frac{\Delta\Omega}{2}, & \Omega_2 &= \Omega_0 + \frac{\Delta\Omega}{2} \\
 \Omega_0 &= \frac{1}{2} \sqrt{(R+1)^2 + \mu_{sl}}, & \Delta\Omega &= \sqrt{(R-1)^2 + \mu_{sl}} \\
 R = \frac{\omega_1}{\omega_2} &= \Omega_1 \Omega_2 \\
 \bar{\omega}_{n1} &= \omega_{n1} \sqrt{1 - \xi_{n1}^2}, & \bar{\omega}_{n2} &= \omega_{n2} \sqrt{1 - \xi_{n2}^2} \\
 \xi_{n1}\omega_{n1} + \xi_{n2}\omega_{n2} &= 2\omega_2\beta, & \xi_{n1}\omega_{n1} - \xi_{n2}\omega_{n2} &= 2\omega_2\theta \\
 \beta &= \frac{1}{2} \left[\xi_1 R + (1 + \mu_{sl}) \xi_2 \right] \\
 \theta &= \left[\frac{\xi_1 R (1 - \Omega_1^2)^2 + \mu_{sl} \xi_2 \Omega_1^4}{(1 - \Omega_1^2)^2 + \mu_{sl}} - \frac{\xi_1 R + (1 + \mu_{sl}) \xi_2}{2} \right]
 \end{aligned} \tag{16}$$

The objective is to determine the maximum value of the displacement $x_2(t)$ relative to the "base motion" $x_1(t)$. The maximum value of $x_2(t)$ is called the "generalized" displacement shock spectra since the "base acceleration" $\ddot{x}_1(t)$ is allowed to be affected by $\ddot{x}_2(t)$, unlike the simple traditional shock spectra concept. To derive relatively simple expressions requiring minimal numerical calculation for the generalized modal displacement spectra, further mathematical simplifications will be introduced in Equations (15) and (16). These simplifications were tested and found accurate when the results below were compared with the results of the analog solution of Appendix A.

First, since ξ_{n1}^2 and ξ_{n2}^2 are much smaller than unity, the approximation

$$\text{for } R \neq 0: \quad \xi_{n1} \doteq \xi_{n2} \doteq \xi_n = \frac{\xi_{n1} + \xi_{n2}}{2} = \frac{1}{\omega_2 R} \left[\Omega_0 \beta + \frac{\Delta \Omega}{2} \right] \quad (17)$$

$$\text{for } R = 0: \quad \xi_n = \frac{\xi_2}{2}$$

is used for the damped natural frequencies $\bar{\omega}_{n1}$ and $\bar{\omega}_{n2}$, so that:

$$\bar{\omega}_{n1} \doteq \omega_2 (\rho_1 - \rho_2) \quad (18)$$

$$\bar{\omega}_{n2} \doteq \omega_1 (\rho_1 + \rho_2) \quad (19)$$

where

$$\omega_2 \rho_1 = \omega_2 \Omega_0 \sqrt{1 - \xi_n^2} = \text{damped center frequency}$$

$$\omega_2 \rho_2 = \omega_2 \frac{\Delta \Omega}{2} \sqrt{1 - \xi_n^2} = \text{damped beat frequency}$$

Note that the approximation of Equation (17) is not used for the exponential part of the solution. Also note $\Delta\Omega/2\Omega_0 = \rho_2/\rho_1$.

Furthermore, according to Equation (16), $\theta \ll \beta$. In fact, θ tends to be exceedingly small in the neighborhood of $R = 1$. Therefore, it is sufficient to retain only the first order approximation for $e^{\theta t}$, i.e., $e^{\theta t} \doteq 1 + \theta t$, and correspondingly $e^{-\theta t} = 1 - \theta t$. This approximation, along with that of Equation (17) and some trigonometric transformations, lead to the following simplified expression for the relative displacement $x_2(t)$ for the spacecraft mode:

$$x_2(\tau) \doteq -\omega_1 v_{0z} [D_1(\tau) + D_2(\tau)], \quad \tau = \omega_2 t \quad (20)$$

where

$$D_1(\tau) = \frac{1}{2\omega_2^2 \rho_2} \left(\frac{\rho_2}{\rho_1} - \theta\tau \right) e^{-\beta\tau} \sin \rho_1 \tau \cos \rho_2 \tau$$

$$D_2(\tau) = \frac{-1}{2\omega_2^2 \rho_1} \left(\frac{\rho_1}{\rho_2} - \theta\tau \right) e^{-\beta\tau} \cos \rho_1 \tau \sin \rho_2 \tau$$

For $R \neq 0$: since ρ_2 is smaller than ρ_1 , an accurate estimate of the maximum value of the relative displacement $x_2(t)$ of Equation (20) is provided by the discrete maxima D_{\max} of the simple sinusoid, where $\cos \rho_1 \tau$ and $\cos \rho_2 \tau$ are either zero or unity, (see Figure 3-1). When $D_1(\tau)$ approaches its maximum $D_{1\max}$, $D_2(\tau)$ approaches zero, and vice versa. Therefore, the maximum relative displacement D_{\max} is given by the largest of $D_{1\max}$ or $D_{2\max}$:

$$\left. \begin{aligned} D_{1\max} &= \frac{1}{2\omega_1^2 \rho_2} \left(\frac{\rho_2}{\rho_1} - \theta\tau \right) e^{-\beta\tau} \sin \rho_1 \tau \\ D_{2\max} &= \frac{1}{2\omega_2^2 \rho_1} \left(\frac{\rho_1}{\rho_2} - \theta\tau \right) e^{-\beta\tau} \sin \rho_2 \tau \end{aligned} \right\} \quad (21)$$

ORIGINAL PAGE IS
OF POOR QUALITY

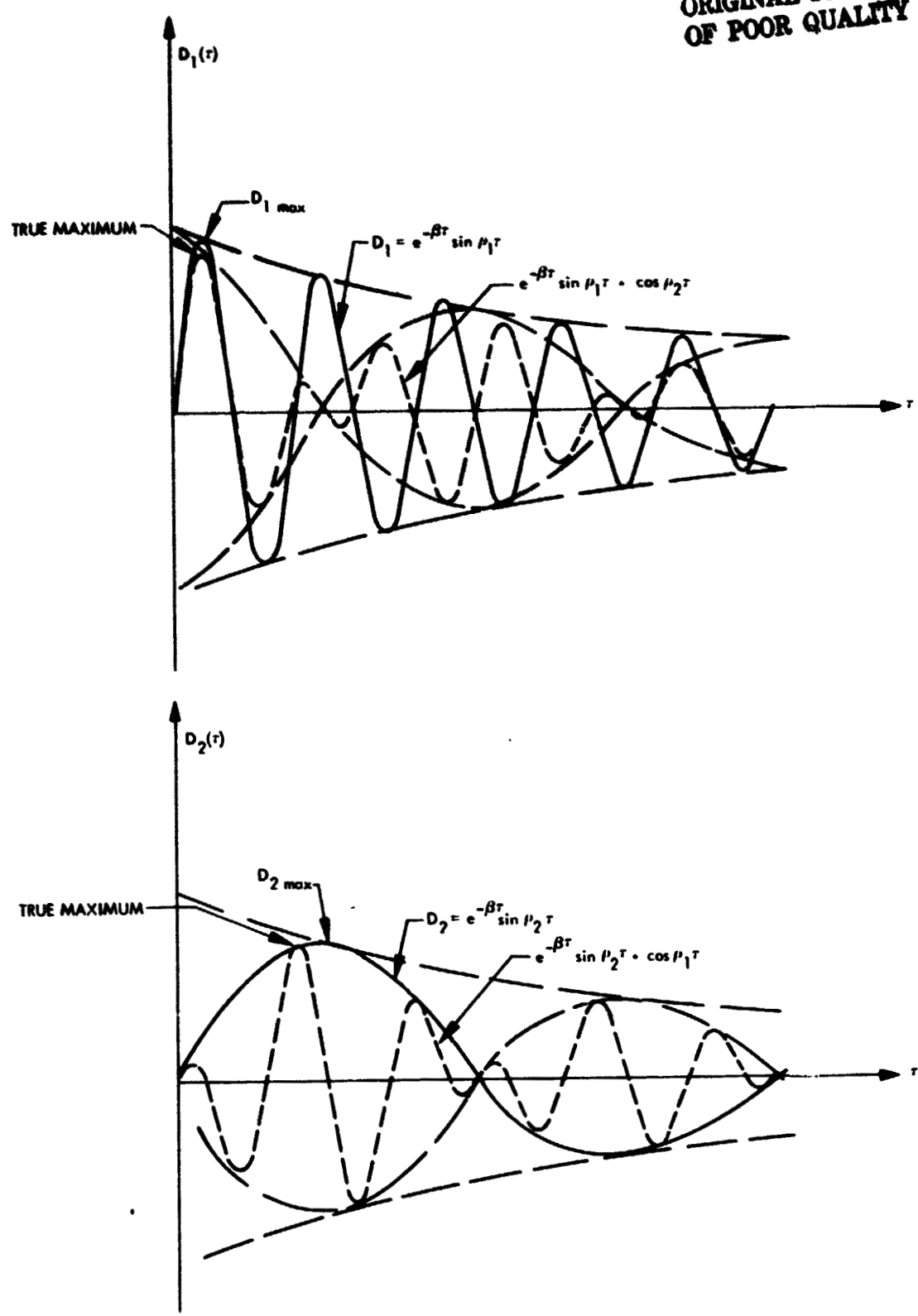


Figure 3-1. Graphic Representation of $D_1(t)$, $D_2(t)$, and Their Approximate Maxima $D_{1 \max}$ and $D_{2 \max}$

where τ is determined as the smallest root of the characteristic equations

$$\text{for } D_{1\text{max}}: \quad \tan \rho_1 \tau = \frac{\rho_1}{\beta} \frac{[1 - (\rho_1/\rho_2) \theta \tau]}{[1 + (\rho_1/\rho_2) \frac{\theta}{\beta} (1 - \beta \tau)]} \quad (22)$$

$$\text{for } D_{2\text{max}}: \quad \tan \rho_2 \tau = \frac{\rho_2}{\beta} \frac{[1 - (\rho_2/\rho_1) \theta \tau]}{[1 + (\rho_2/\rho_1) \frac{\theta}{\beta} (1 - \beta \tau)]}$$

The definitions introduced in Equation (14) and the equalities of Equations (21) and (22) are now combined to give the generalized modal displacement spectra, Q_{sl} :

$$Q_{sl} = \left| \frac{\omega_1 v_{0l} \sqrt{m_{sl}}}{(1 + M_{sl})} D_{\text{max}} \right| \quad (23)$$

Equation (23) above, along with its companion expressions of Equations (21) and (22) represent a generalization of the traditional shock spectra concept since these expressions account for interactions between the oscillator and its base, i.e., between the spacecraft and launch vehicle modes. They also represent an improvement over the results of Reference 1-2 in that they hold true for an arbitrary pair of coupled modes, a launch vehicle mode and a spacecraft mode, regardless of the proximity of their respective natural frequencies. It is this fact that makes it possible in the present approach to include contributions of all launch vehicle and spacecraft modes in the computation of bounds on the modal displacements and subsequently on the member loads. It is noted here that Equation (21) suggests that the damping effect is through the "average" damping β of the spacecraft and the launch vehicle as defined in Equations (16) rather than through each damping separately. This point is explained further in Appendix A. Although derived for $R \neq 0$, Equation (23) is still valid in the limit for $R \rightarrow 0$. This is shown in Appendix D.

The generalized shock spectra will be identical to the traditional shock spectra in the limit when, in Equation (23), the mass ratio, μ_{sl} defined by Eq. (14) for the oscillator equivalent spacecraft mode, is allowed to approach zero while the associated stiffness increases such that the natural frequency is held unaltered. This is the case of the shock spectrum of a rigidly-loaded launch vehicle mode. This remark will be useful subsequently, in evaluating the initial velocity v_{0l} of Equation (23).

Generally, however, for each set of parameters $R, \omega_1, \xi_1, \xi_2, \mu_{sl}, \dots$, etc, describing the characteristics of a spacecraft mode s , and a launch vehicle mode l , Equations (21), (22), and (23) will yield an estimate of the upper bound of the corresponding generalized modal displacement spectrum, Q_{sl} , in terms of the as-yet unknown initial modal velocity, v_{0l} . Once v_{0l} has been determined, the generalized modal displacement spectra, Q_{sl} , for $s = 1, 2, \dots S$, and $l = 1, 2, \dots L$ can be combined to establish a bound for the member loads.

C. DETERMINATION OF THE INITIAL MODAL VELOCITY v_{0l}

An analysis of the launch vehicle with some representation of the spacecraft is usually done by the launch vehicle organization for the structural design of the launch vehicle, or part of it. To properly design the part of the launch vehicle at the interface with the spacecraft, the reaction loads from the spacecraft to the launch vehicle must be introduced in the analysis. Since these loads are almost entirely due to the fundamental cantilevered modes of the spacecraft, a simple model of the spacecraft such as a two-mass model is adequate. Note that this simple spacecraft model is used for the design of the launch vehicle at its interface with the spacecraft, but is not intended to be used for the detail design of the spacecraft. However, this two-mass model is useful for checking the launch vehicle data and can also be used to determine the weighting factor W_l defined later.

The original launch vehicle forcing functions as used for the launch vehicle analysis are given by a set of components $\{F_j(t)\}$ expressed in the physical coordinate system xyz and applied at given locations of the launch vehicle structure. The modal analysis done on the launch vehicle with any spacecraft or dummy provides, in effect, a new system of coordinates, i.e., the generalized coordinates $q_c(t)$, that are used to express new components of the forcing functions as a set of generalized forces $F_c(t)$. In effect, $F_c(t)$ is another definition of the same forcing functions $F_j(t)$. Therefore, one can use this set $\{F_c(t)\}$ to represent the forcing functions without the need of knowing the physical components, nor the location of the original forcing functions. Note that this observation holds only because an analysis of the launch vehicle with a dummy spacecraft has already been done.

Any further change of modes, if necessary, will simply change the set $\{F_c(t)\}$ by a modal transformation. For example, the present method requires the use of the modes of the launch vehicle loaded only by a rigid mass. Therefore, the components $\{F_\ell(t)\}$ of the forcing functions with respect to the rigid mass loaded launch vehicle modes are

$$\{F_\ell(t)\} = [V^T]\{F_c(t)\} \quad (24)$$

where $[V]$ is the modal matrix that transforms the elastically loaded launch vehicle to the rigid-mass loaded one as shown in Appendix C.

Similarly, the generalized coordinates $\{\ddot{q}_\ell(t)\}$ of the rigid mass loaded launch vehicle are obtained from the coordinates $\{\ddot{q}_c(t)\}$ of the elastically loaded launch vehicle by Equation (C-18) or Equation (C-20) of Appendix C.

The unknown initial modal velocity $v_{0\ell}$ can be determined from the requirement that the "actual" forcing function and the "idealized" forcing function produce identical bounds for the modal displacement spectra. Information for the "actual" forcing function can be obtained either from an initial analysis done on a simplified model of the spacecraft-launch vehicle combination, or from recorded flight response data for another spacecraft. It is believed that the minimum required

information is three degrees of freedom at the spacecraft-launch vehicle interface. The knowledge of more degrees of freedom improves the definition of v_{0l} . In case of an available initial analysis, the knowledge of the modal response-time histories for each mode leads to the best estimate of v_{0l} . For the last case, the peak value of the traditional displacement shock spectra, D_l^P , is calculated for the modal acceleration response $\ddot{q}_l(t)$ of the rigid mass loaded launch vehicle as shown by Equations (28) and (29).

Finally, it should be noted that D_l^P will need to be computed only once for each launch vehicle mode and each flight event of interest. This part of the computation will remain the same as long as the launch vehicle and the forcing functions are not changed.

In the derivation done so far and in what follows, rigid mass loaded launch vehicle modes are used. These modes are obtained by the method of Appendix C, or directly from the launch vehicle analysis if the spacecraft was represented by a rigid mass, as may be the case for preliminary launch vehicle design.

1. Estimate of v_{0l} From the Modal Response

Assuming now that the time histories $\ddot{q}_l(t)$, $l = 1, 2, \dots, L$ for the rigidly-loaded launch vehicle are available from a previous launch vehicle analysis, and that $D_l^P(\omega_2, \xi_2)$ representing the peak of the modal displacement spectrum $D_l(\omega_2, \xi_2)$ for each mode has been evaluated, then v_{0l} can be determined by requiring that D_l^P be equal to its counterpart, Q_l^P , derived from Equation (23) for $\mu_{sl} \rightarrow 0$. This is illustrated in Figure 3-2. To derive Q_l^P for $R \neq 0$, the shock spectrum Q_l is computed for each of the launch vehicle elastic modes $l = 7, 8, \dots, L$ from Equation (23) in the limit as $\mu_{sl} \rightarrow 0$. Appendix D gives the proper values of the modal shock spectra for the case when $R = 0$, that is, for $l = 1, \dots, 6$.

$$Q_l = \left| \omega_1 v_{0l} \lim_{\mu_{sl} \rightarrow 0} (D_{\max}^P) \right| \quad (25)$$

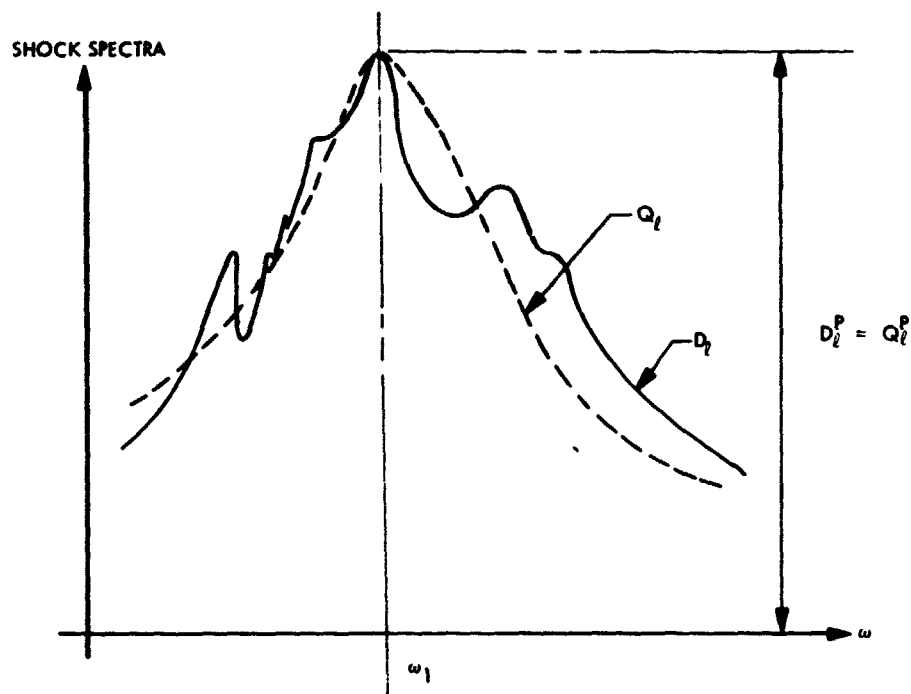


Figure 3-2. Modal Displacement Spectra D_l and Q_l for a Launch Vehicle Mode l

The quantity, $\lim_{\mu_{sl} \rightarrow 0} (D_{\max})$, of Equation (25) is readily evaluated by substituting the following parameters in Equations (21) and (22): as $\mu_{sl} \rightarrow 0$, and $R \neq 0$

$$\begin{aligned}
 \beta &= \frac{1}{2} (\xi_1 R + \xi_2) \\
 \theta &= \frac{1}{2} (\xi_1 R - \xi_2) \\
 \frac{2\Omega_0}{\Delta\Omega} &= (R + 1)/(R - 1) \\
 \rho_1 &= \frac{1}{2} (R + 1) \sqrt{1 - \xi_n^2} \\
 \rho_2 &= \frac{1}{2} (R - 1) \sqrt{1 - \xi_n^2} \\
 \xi_n &= \frac{1}{2} (\xi_1 + \xi_2)
 \end{aligned}
 \tag{26}$$

As seen from Equation (26), the displacement shock spectrum of Equation (25) is dependent upon the value of $R = \omega_1/\omega_2$. The peak value of Q_ℓ , labeled Q_ℓ^P , occurs for $R \rightarrow R^P$. Finding the exact value of R^P that maximizes Q_ℓ is rather involved analytically. Only an approximate estimate will be given here.

Considering the special case when θ and ξ_n^2 of Equation (26) are assumed negligibly small, we find that

$$\lim_{\mu_{sl} \rightarrow 0} (D_{\max}) = R \frac{e^{-[\tan^{-1} (a_r/2\beta)/(a_r/2\beta)]}}{\omega_2^2 \sqrt{a_r^2 + 4\beta^2}}, \quad (r = 1, 2) \tag{27}$$

where

$$a_r = \begin{cases} (R + 1) & \text{for } r = 1 \\ (R - 1) & \text{for } r = 2 \end{cases}$$

By inspection of Equation (27), it is concluded that the peak occurs for $r = 2$ and $R^P = 1$. The approximation that θ in Equation (26) is negligibly small, is of the same order as the approximation that the imaginary part of the solution of Equation (15) is negligible, both of which are acceptable. The exact solution was evaluated from the analog simulation of Appendix A, in which the maximum of D_{\max}^P occurred within better than 1% from $R = 1$. For $R^P = 1$, Equations (25) and (26) yield the following expression for the initial modal velocity and for $\omega_1 \neq 0$:

$$\omega_1 v_{0l} = e \omega_1^2 (\xi_1 + \xi_2) D_l^P(\omega_2, \xi_2) \quad (28)$$

where $e = 2.718$.

Instead of the modal displacement peak $D_l^P(\omega_2, \xi_2)$, the modal acceleration peak $A_l^P(\omega_2, \xi_2)$ may be used. At the peak of the displacement, the two quantities are related by $\omega_2^2 D_l^P(\omega_2, \xi_2) = A_l^P(\omega_2, \xi_2)$. Thus, the following alternate expression for v_{0l} is used, noting that $\omega_1 = \omega_2$:

$$\omega_1 v_{0l} = e (\xi_1 + \xi) A_l^P(\omega_2, \xi) \quad (29)$$

for $\omega_1 \neq 0$ and where ξ is the damping used in calculating the acceleration shock spectra A_l of $\ddot{q}_l(t)$.

As shown in Appendix D, for $\omega_1 = 0$ Equation (29) becomes

$$(\omega_1 v_{0l})_{\omega_1 \rightarrow 0} = A_l^P$$

2. Estimate of v_{0l} From Physical Interface Response

In the absence of availability of $\ddot{q}_c(t)$, a set of initial modal velocities v_{0l} can also be obtained in a manner similar to that of

Reference 3-1. It is assumed that the time histories from an analysis or flight data of an N_0 degrees of freedom at the launch vehicle/spacecraft interface are known for another spacecraft or a dummy one. The shock spectra S_i ($i = 1, 2, N_0$) for the N_0 degrees of freedom are calculated, as typically represented by the solid line of Figure 3-3.

Next it is assumed that the mode shapes ϕ_n of the structure corresponding to the available interface acceleration are also known. Then each mode is given an initial velocity v_{On} and the total interface acceleration is calculated from:

$$\ddot{R}_i(t) = - \sum_{n=1}^N \omega_n v_{On} \phi_n e^{-\xi_n \omega_n t} (a_n \sin \omega_d t + b_n \cos \omega_d t) \quad (30)$$

where

$$a_n = (1 - 2\xi_n^2) / \sqrt{1 - \xi_n^2}$$

$$b_n = 2\xi_n$$

$$\omega_d = \omega_n \sqrt{1 - \xi_n^2}$$

The value of v_{On} can be determined by trial and error so that the shock spectra of $\ddot{R}_i(t)$ above, represented by the dashed line in Figure 3-3, envelopes the shock spectra of the real response. Since only a small number of vehicle modes are significantly contributing to \ddot{R}_i , one can choose a set of modes $\bar{N} < N$ to simplify the calculations. The important criteria is that the v_{On} and the mode retained give an envelope of the real shock spectra.

Finally, the initial modal velocity v_{Ol} for the rigid mass loaded launch vehicle is obtained by the transformation of Equation (31), where a bound for v_{Ol} will be obtained by taking root sum square values, since the sign of v_{On} is not retained.

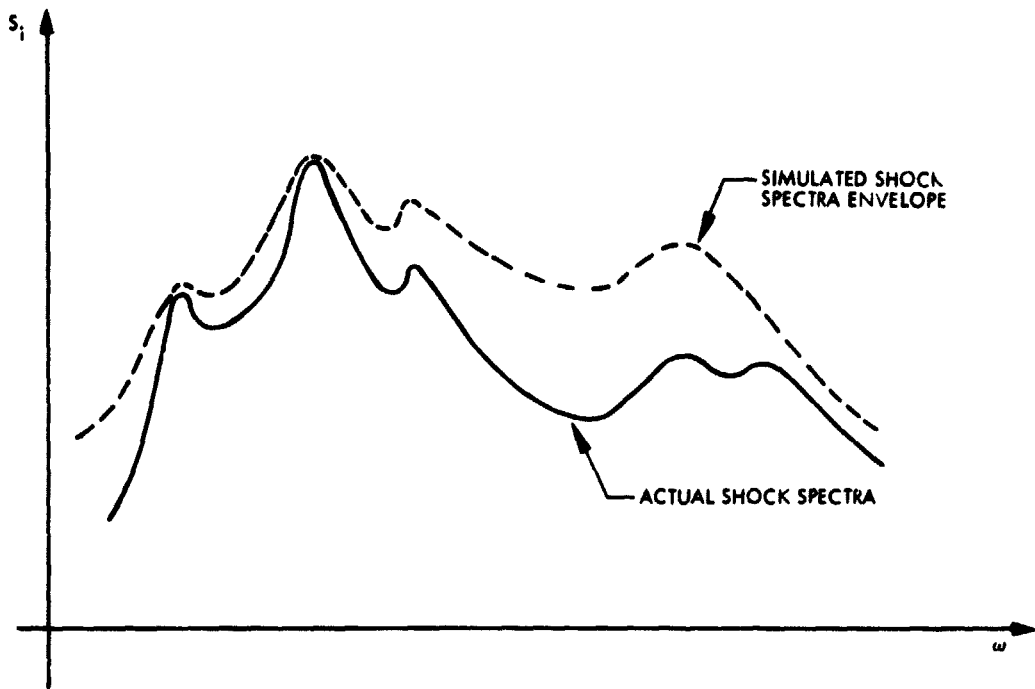


Figure 3-3. Shock Spectra Matching and Envelope

$$\{\omega_1 v_{0l}\} = \left[\sqrt{\sum_n (v_{ln} \omega_n v_{0n})^2} \right] \quad (31)$$

Note that this method is only a fall-back method, and that the modal response method of the previous section is to be preferred.

D. TUNING

During the early stages of design, the spacecraft and launch vehicle modes and frequencies are obtained from analyses that usually contain a large degree of uncertainty. To account for such uncertainties, one may introduce an artificial tuning between the spacecraft and launch vehicle modes. Unlike other methods, the present approach makes artificial tuning possible and easy to implement because Equation (23) is inexpensive to evaluate and is valid for any pair of spacecraft and launch vehicle modes, regardless of the proximity of their respective frequencies.

Two forms of artificial tuning have been identified: global and local. In global tuning, the entire spectrum of launch vehicle frequencies is incrementally scaled in either direction relative to the spacecraft frequency spectrum. For each increment, a global response

$$\bar{Q} = \sqrt{\sum_l \sum_s Q_{sl}^2}$$

is computed and used as a measure for determining the worst case for design purposes. In this scheme, tuning is achieved by finding the amount of relative scaling that maximizes \bar{Q} . Clearly, limits on the allowable relative scaling must be selected in advance, and the search for the maximum \bar{Q} conducted within these limits.

In the local tuning, the response is maximized for each spacecraft mode, one at a time. This is achieved by allowing the nearest launch vehicle frequency to coincide with that of the spacecraft frequency

under consideration, (i.e., $R \rightarrow 1$) provided that the two were originally separated by no more than a preselected amount. Other schemes for tuning can be also devised.

ORIGINAL PAGE IS
OF POOR QUALITY

SECTION IV

SPACECRAFT MEMBER LOADS, DISPLACEMENTS, AND ACCELERATION

A. MEMBER LOADS

When the time histories of the spacecraft generalized modal displacement $q_s(t)$ are determined as a result of a transient analysis, one can express the vector of the spacecraft modal member loads, $\{f_{as}(t)\}_A$, for each member A due to motion in mode s in the general form (Reference 2-1):

$$\{f_{as}(t)\}_A = [C_{ab}]\{\phi_{bs}\} q_s(t) \quad (32)$$

where

$$s = 1, 2, \dots, S$$

In addition, the total load vector due to contributions of all spacecraft modes is

$$\{f_a(t)\}_A = \sum_{s=1}^S \{f_{as}(t)\}_A \quad (33)$$

where

$[C_{ab}]_A$ = matrix of force coefficients, whose elements are the a^{th} force component in member A due to a unit displacement in the b^{th} degree of freedom

$\{\phi_{bs}\}$ = as before, spacecraft mode shape at the b^{th} degree-of-freedom

$[C_{ab}]\{\phi_{bs}\}$ = is recognized as the vector of modal stresses for mode s.

In the present approach, the time histories of the spacecraft generalized modal displacements $q_s(t)$ in Equations (32) and (33) are

not computed for the entire $(S + L)$ mathematical space. Instead, they are replaced by an estimate of their upper bound, Q_s , so that the corresponding bound on the spacecraft modal member loads, $\{F_{as}\}_A$ is written analogous to Equation (32) in the form:

$$\{F_{as}\}_A = [C_{ab}]_A \{\phi_{bs}\} Q_s \quad (34)$$

The bound, Q_s , for the spacecraft generalized modal displacement is expressed in terms of the discrete modal displacement spectra, Q_{sl} of Equation (23) for each of the $(S \times L)$ discrete mathematical subspaces. Since each Q_{sl} results from coupling between a spacecraft mode s and only one launch vehicle mode, and since a complete representation of the launch vehicle includes more than one mode, say L modes, contributions due to all L modes should be included. Clearly, because Equation (23) does not contain information regarding time-phasing among modes, only a bound can be computed, and is provided by summation over absolute values or in the root-sum-square sense.

Thus, Q_s is estimated by

$$Q_s = \sum_{l=1}^L |Q_{sl}| \quad (35)$$

or

$$Q_s = \sqrt{\sum_{l=1}^L Q_{sl}^2} \quad (36)$$

or

$$Q_s = \sqrt{\sum_{l=1}^L [W_l(\omega_s, \omega_l) Q_{sl}]^2} \quad (37)$$

ORIGINAL PAGE IS
OF POOR QUALITY

where $W_s(\omega_s, \omega_l)$ is a weighting function that can be used to account for time phasing between the launch vehicle modes. This weighting function can be determined from the available transient response of the simplified two-mass model of the spacecraft or from matching of the shock spectra of the mass-loaded launch vehicle interface.

Analogous to the calculation of Q_s , a bound on the magnitude of the total vector of member loads $\{F_a\}_A$ due to all spacecraft modes $s = 1, 2, \dots, S$ is found from:

$$\{F_a\}_A = \left\{ \sum_{s=1}^S |F_{as}| \right\} \quad (38)$$

or

$$\{F_a\}_A = \left\{ \sqrt{\sum_{s=1}^S F_{as}^2} \right\} \quad (39)$$

or

$$\{F_a\}_A = \left\{ \sqrt{\sum_{s=1}^S [W_s(\omega_s) F_{as}]^2} \right\} \quad (40)$$

Member loads computed by Equations (35) and (38) are, of course, much more conservative than those computed by Equations (36), (37), (39), and (40). Such excessive conservatism may be unnecessary, especially if each Q_s for a spacecraft mode s is artificially tuned to the nearest launch vehicle mode.

B. DISPLACEMENTS AND ACCELERATIONS

An estimate of the bound on the displacements and accelerations associated with any or all degrees-of-freedom used in the spacecraft

model can be obtained in a manner similar to the member loads of Equation (34). Once Q_s has been established according to Equations (35), (36), or (37), a bound on the spacecraft modal relative displacements $\{D_{bs}\}$, or absolute accelerations $\{A_{bs}\}$, are found, respectively from:

$$\{D_{bs}\} = \{\phi_{bs}\} Q_s \quad (41)$$

$$\{A_{bs}\} = \omega_s^2 \{\phi_{bs}\} Q_s \quad (42)$$

Finally, a bound on the spacecraft total displacement and acceleration degrees of freedom, $\{D_b\}$ and $\{A_b\}$, is written analogous to Equations (38) through (40). For the displacements,

$$\{D_b\} = \left\{ \sum_{s=1}^S |D_{bs}| \right\} \quad (43)$$

or

$$\{D_b\} = \left\{ \sqrt{\sum_{s=1}^S D_{bs}^2} \right\} \quad (44)$$

or

$$\{D_b\} = \left\{ \sqrt{\sum_{s=1}^S [W_s(\omega_s) D_{bs}]^2} \right\} \quad (45)$$

Similarly, for the accelerations,

ORIGINAL PAGE IS
OF POOR QUALITY

$$\{A_b\} = \left\{ \sum_{s=1}^S |A_{bs}| \right\} \quad (46)$$

or

$$\{A_b\} = \left\{ \sqrt{\sum_{s=1}^S A_{bs}^2} \right\} \quad (47)$$

or

$$\{A_b\} = \left\{ \sqrt{\sum_{s=1}^S [W_s(\omega_s) A_{bs}]^2} \right\} \quad (48)$$

C. FLOW DIAGRAM

Figure 4-1 summarizes the different steps taken from the launch vehicle data to the computation of bounds for the member loads, displacements, and accelerations.

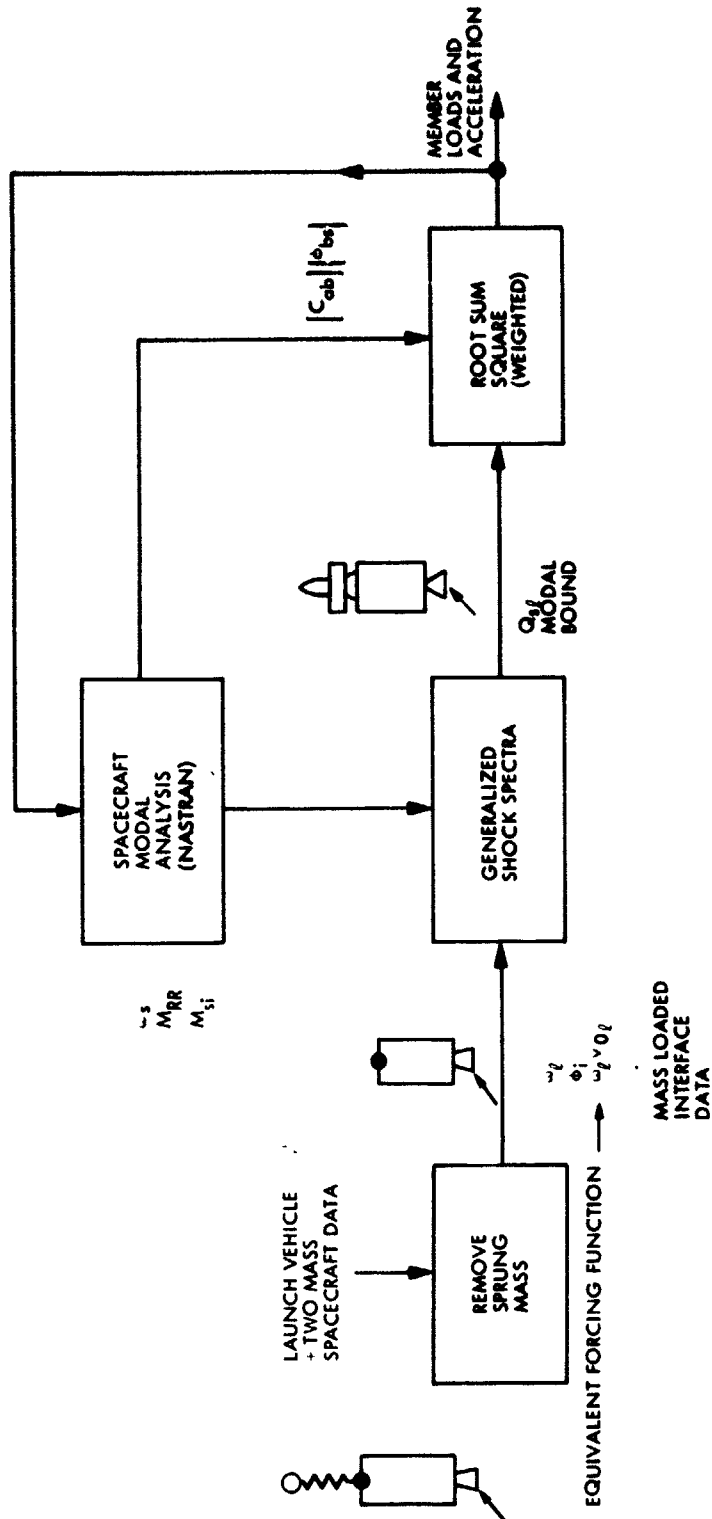


Figure 4-1. Generalized Shock Spectra Method

SECTION V
CONCLUSIONS

ORIGINAL PAGE IS
OF POOR QUALITY

The primary drawback of the original shock spectra method (Reference 1-1) is that it can result in very conservative answers, and therefore overdesign. It is also very dependent upon the analyst's judgment. However, it has the advantage of low cost of analysis and yields bounds that can be readily used for design. The transient analysis, on the other hand, is accurate, but is very expensive and difficult to implement because of its sensitivity to design change. The generalized shock spectra approach described in this paper, although still an approximate procedure, combines the advantages of low cost while maintaining a very reasonable accuracy. In addition, unlike the method of Reference 1-1, it is substantially less dependent upon the analyst's intuitive judgment in pairing spacecraft and launch vehicle modes. Because of its low cost, the tuning effect of launch vehicle modes with spacecraft mode can be very easily explored and used for design to establish worst case. Finally, the procedure is currently being applied to the Galileo spacecraft loads analysis with very acceptable results.

PRECEDING PAGE BLANK NOT FILMED

REFERENCES

- 1-1. Chen, J., J. Garba, and B. Wada, "Estimation of Payload Loads Using Rigid Body Interface Accelerations," paper No. 78-519, presented at the 19th Structures, Structural Dynamics, and Materials Conference, Bethesda, Maryland, April 1978.
- 1-2. Bamford, R., and M. Trubert, "A Shock Spectra and Impedance Method to Determine a Bound for the Spacecraft Structural Loads," Technical Memorandum 33-694, Jet Propulsion Laboratory, California Institute of Technology, September 1974.
- 1-3. Garba, J., B. Wada, R. Bamford, and M. Trubert, "Evaluation of a Cost-Effective Loads Approach," Journal of Spacecraft and Rockets, Vol. 23, No. 11, Nov. 1976, pp. 675-683.
- 2-1. Hurty, W., "Dynamic Analysis of Structural Systems Using Component Modes," AIAA Journal, vol. 3, No. 4, 1965, pp. 678-685.
- 2-2. Wada, B., R. Bamford, and J. Garba, "Equivalent Spring-Mass System: A Physical Interpretation," The Shock and Vibration Bulletin, January, 1972, pp. 215-225.
- 3-1. Trubert, M., and A. Egwuatu, "Helios TC-2 Stage Zero Ignition Pulse Reconstruction for MJS'77 Loads Analysis," Project Document 618-426, Jet Propulsion Laboratory, Pasadena, Calif., August 1976. (JPL internal document.)

APPENDIX A

ANALOG SOLUTION OF THE EQUATIONS OF MOTION

PRECEDING PAGE BLANK NOT FILMED

The analog exact solution of Equation (13) is given here to verify the analytical solution of Equation (15) and Appendix B. The equations of motion for the free vibration of the system in Equation (13), or that of Figure A-1, are

$$(1 + \mu) \ddot{x}_1 + \mu \ddot{x}_2 + 2\xi_1 \omega_1 \dot{x}_1 + \omega_1^2 x_1 = 0 \quad (\text{A-1})$$

$$\mu \ddot{x}_1 + \ddot{x}_2 + 2\mu \xi_2 \omega_2 \dot{x}_2 + \mu \omega_2^2 x_2 = 0 \quad (\text{A-2})$$

where

μ = ratio of a spacecraft mode effective mass m_2 to a launch vehicle mode corrected effective mass m_1 ; also, $\mu = \mu_{sl}$ of Equation (13)

ω_1 = corrected natural frequency of one launch vehicle mode

ω_2 = cantilevered natural frequency of a spacecraft mode

ξ_1 = launch vehicle modal damping

ξ_2 = spacecraft modal damping

x_1 = mass 1 response (unit mass)

x_2 = mass 2 response (mass μ)

The solution of Equations (A-1) and (A-2) to an impulse force applied on mass 1 is sought. Equivalently, the initial conditions for Equations (A-1) and (A-2) are

$$\dot{x}_1(0) = F_0 \quad \dot{x}_2(0) = 0 \quad (\text{A-3})$$

$$x_1(0) = 0 \quad x_2(0) = 0$$

where F_0 is a constant.

To apply the initial conditions of Equation (A-3), the right hand side of Equations (A-1) and (A-2) must be

$$F_1 = (1 + \mu) F_0 \delta(t) \quad (\text{A-4})$$

$$F_2 = \mu F_0 \delta(t)$$

Figure A-2 shows the analog diagram corresponding to Equations (A-1) and (A-2) solved by applying initial conditions of Equation (A-3). Figure A-3 shows the analog diagram corresponding to Equations (A-1) and (A-2) solved by applying the impulse forces of Equation (A-4). These two circuits have been shown to give identical response time histories. All the results shown here have been obtained using Figure A-3.

The following parametric variations were made:

- (1) Frequency ratio:

$$\frac{f_2}{f_1} = \frac{\omega_2}{\omega_1} = r = \frac{1}{R}$$

f_1 was held at 50.00 Hz and f_2 was varied from 40.00 Hz to 60.00 Hz.

- (2) Dampings: $\xi_1 = 0.01, 0.02, 0.03$ and $\xi_2 = 0.01, 0.02, 0.03$ maintaining $\xi_1 + \xi_2 = \text{constant} = 0.04$.
- (3) Mass ratio: $\mu = 0, 0.001, 0.01, 0.1, 1.0$.

Figure A-4 shows an example of the time histories of the spring force per unit mass $\omega_2^2 x_2(t)$ for mass 2 versus time for all the parameters R , ξ_1 , ξ_2 , and μ . The quantity of interest for structural loads is the largest peak value $\omega_2^2 D_{\max}$ of $\omega_2^2 x_2(t)$ of mass 2, which is also the peak of the total acceleration a_m of mass 2. The peak value was read from figures similar to Figure A-4. Figure A-5 is an example of plots of the peak value $\omega_2^2 D_{\max}$ versus the frequency ratio R . The results for various values of the mass ratio μ and dampings ξ_1 and ξ_2 , keeping $\xi_1 + \xi_2 = 0.04$ are tabulated in Table A-1.

The solid curve on Figure A-5 has been obtained from a simplified Equation (23) where $\theta = 0$ and where ξ_n has been dropped in the damped natural frequencies $\bar{\omega}_n$.

$$a_m = \omega_2^2 D_{\max} = \omega_1 F_0 \frac{1}{\sqrt{\Delta\Omega^2 + 4\beta^2}} e^{-\alpha(2\beta/\Delta\Omega)} \quad (\text{A-5})$$

where

$$\Delta\Omega = \sqrt{\mu + (1 - R^2)}$$

$$2\beta = \xi_1 R + (1 + \mu) \xi_2$$

$$\alpha = \tan^{-1} (\Delta\Omega/2\beta)$$

$$R = \omega_1/\omega_2$$

In addition,

$$\sin \rho_2 \tau \doteq \sin \frac{\Delta\Omega}{2} \tau = \frac{\tan \frac{\Delta\Omega}{2} \tau}{\sqrt{1 + \tan^2 \frac{\Delta\Omega}{2} \tau}}$$

has been used to show that the results depend on the square root of the mass ratio μ since $\Delta\Omega$ contains μ . The conclusions are as follows:

- (1) For a given value of mass ratio μ , the maximum acceleration occurs for almost equal frequencies $\omega_1 = \omega_2$ as is evident from Figure A-5.
- (2) Within an error of 1% or less, the peak acceleration depends on the sum $\xi_1 + \xi_2$ and not on each separate damping.
- (3) The solid curve on Figure A-5 shows that Equation (A-5) is an excellent estimate of the peak value of the acceleration.

The reduction factor C as defined in Reference 1-2 can be obtained as follows:

$$C = \frac{a_m(\mu \neq 0)}{a_m(\mu = 0)} \quad (A-6)$$

from the analog data of Table A-1.

ORIGINAL PAGE IS
OF POOR QUALITY

It can also be calculated by substituting Equation (A-5) into Equation (A-6).

$$C = \frac{(\xi_1 + \xi_2)}{\sqrt{\Delta\Omega^2 + 4\beta^2}} e^{1-\alpha \cdot (2\beta/\Delta\Omega)} \quad (A-7)$$

where $\Delta\Omega$, β , and α are defined as for Equation (A-5). Equation (A-7) provides the frequency dependence for C.

Figure A-6 shows a comparison between the analog data and Equation (A-7) as a function of μ for various dampings ξ_1 and ξ_2 , keeping $\xi_1 + \xi_2 = 0.04$, and for $R = 1$. This figure shows that Equation (A-7) is a very good estimate of C and that C is virtually independent of the makeup of the sum $\xi_1 + \xi_2$. Only one curve is shown for C as calculated by Equation (A-7). This is true because the value of C, when ξ_1 and ξ_2 are varied while keeping $\xi_1 + \xi_2 = 0.04$, gives a difference too small to be plotted.

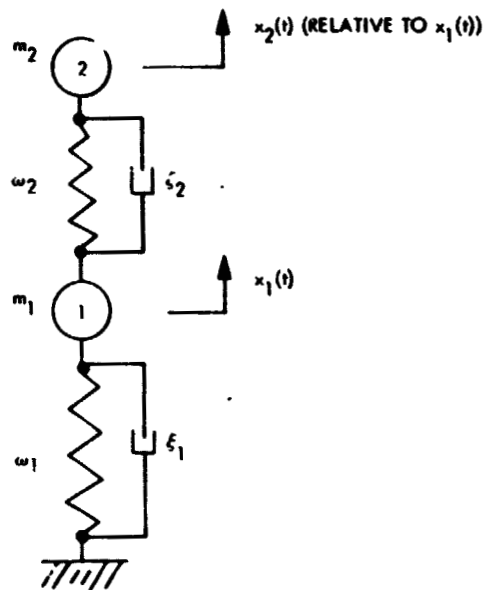


Figure A-1. Launch Vehicle - Spacecraft Modal Model

ORIGINAL PAGE IS
OF POOR QUALITY

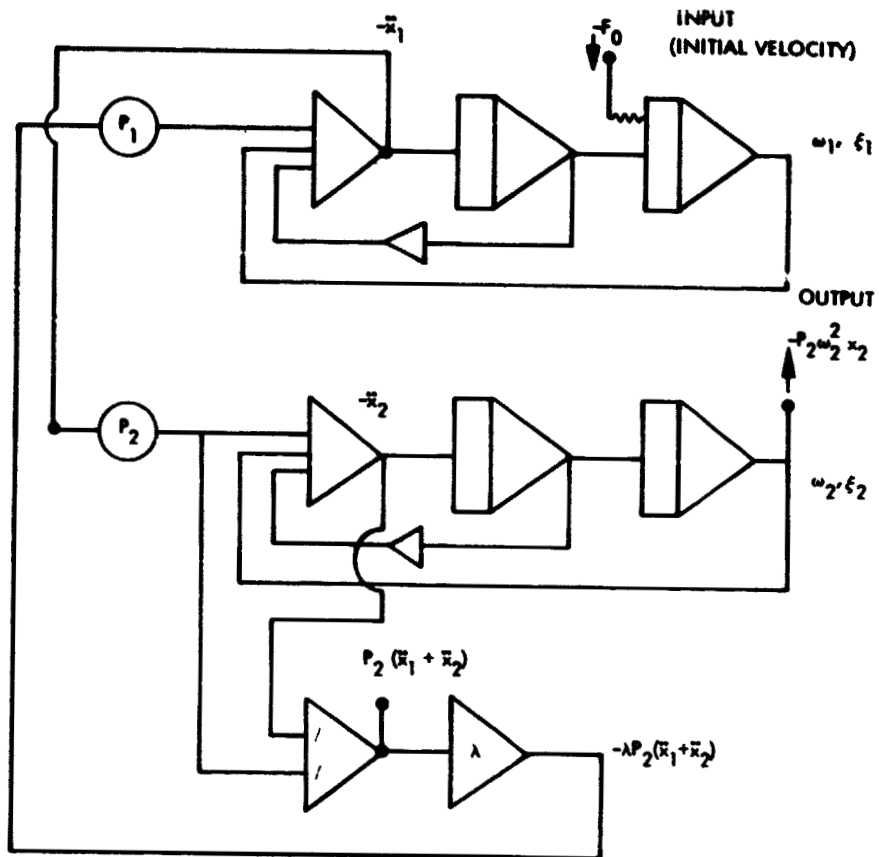


Figure A-2. Analog Schematic for Initial Velocity Solution

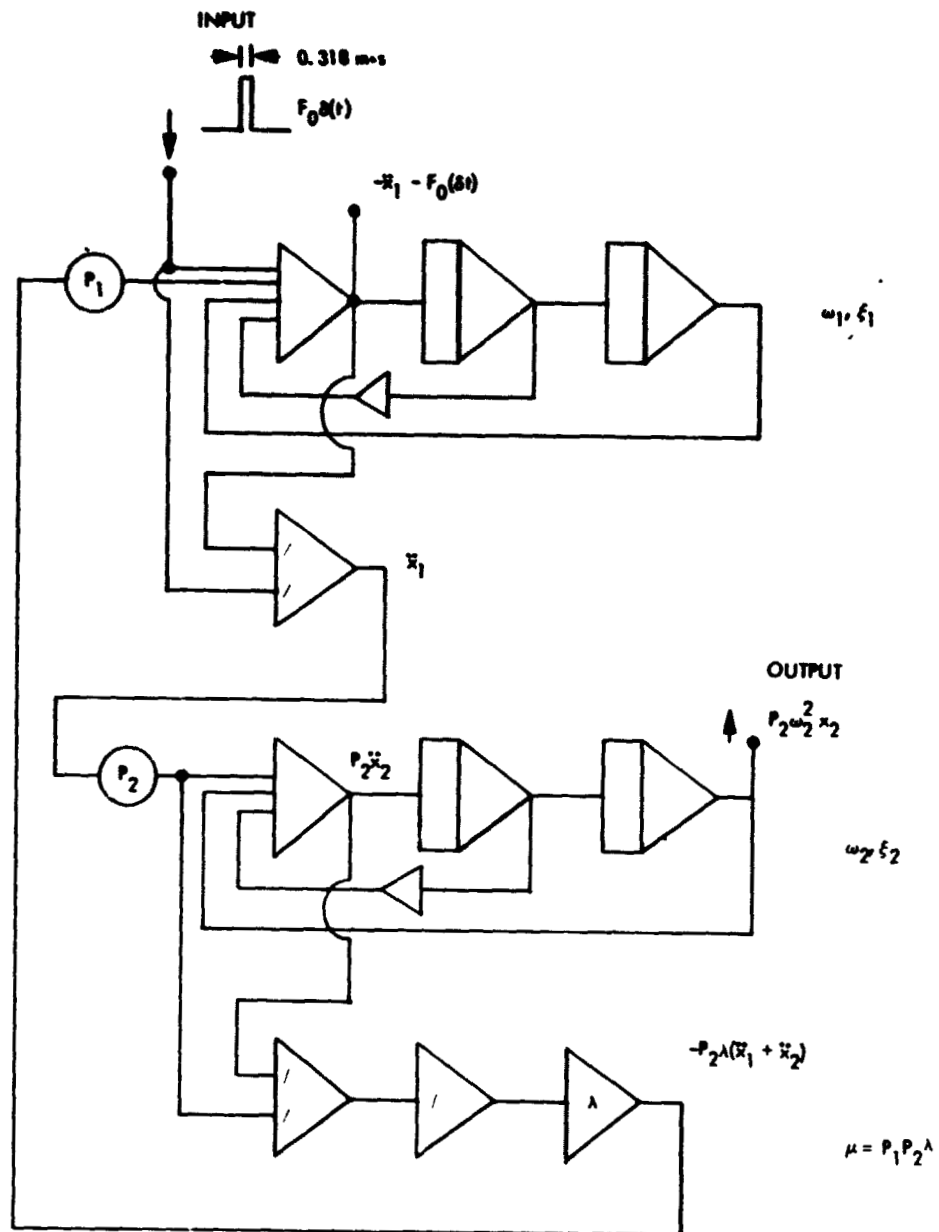


Figure A-3. Analog Schematic for Impulse Solution

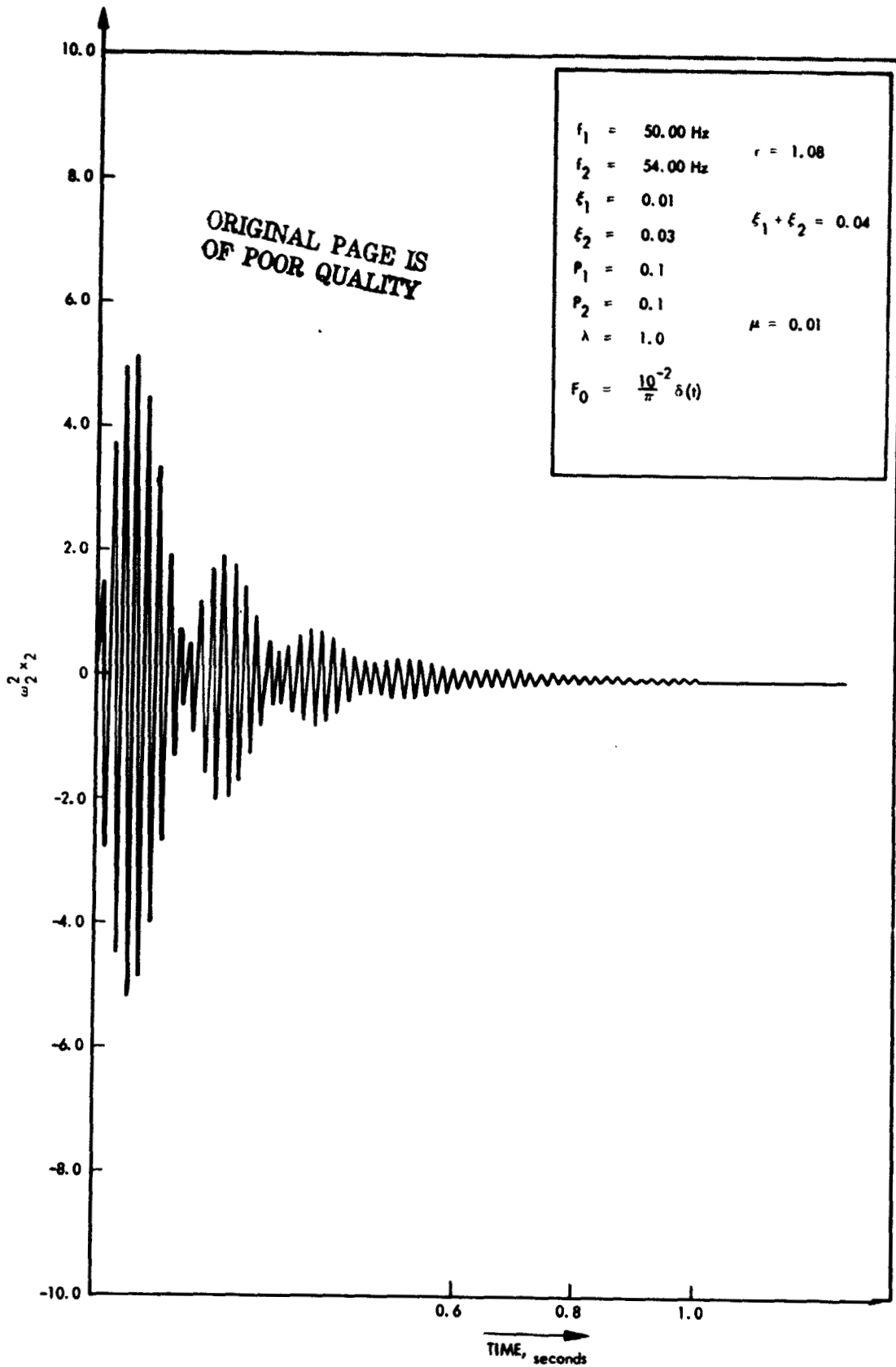


Figure A-4. Mass Number 2 Response to Unit Impulse

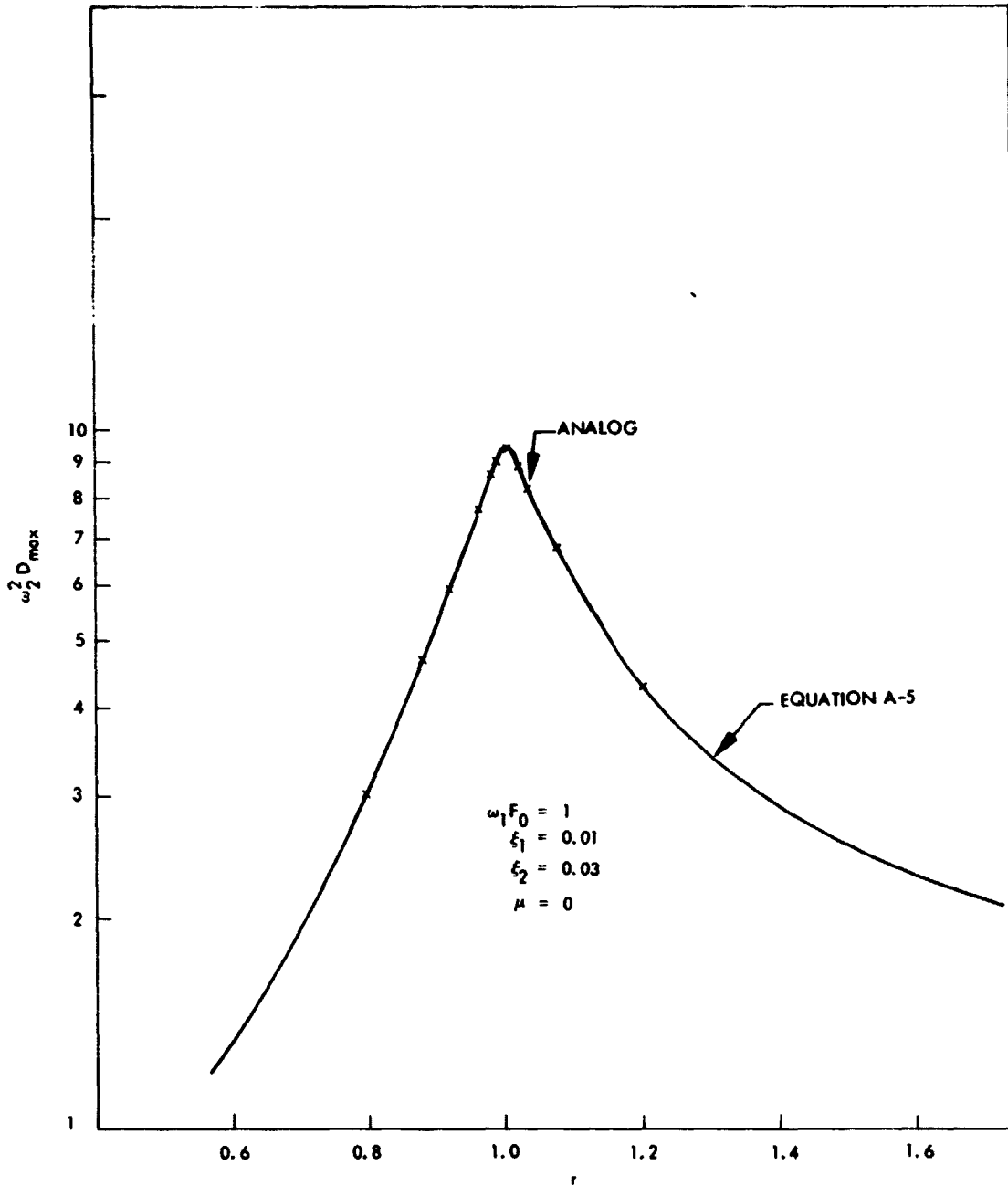


Figure A-5. Generalized Shock Spectra

ORIGINAL PAGE IS
OF POOR QUALITY

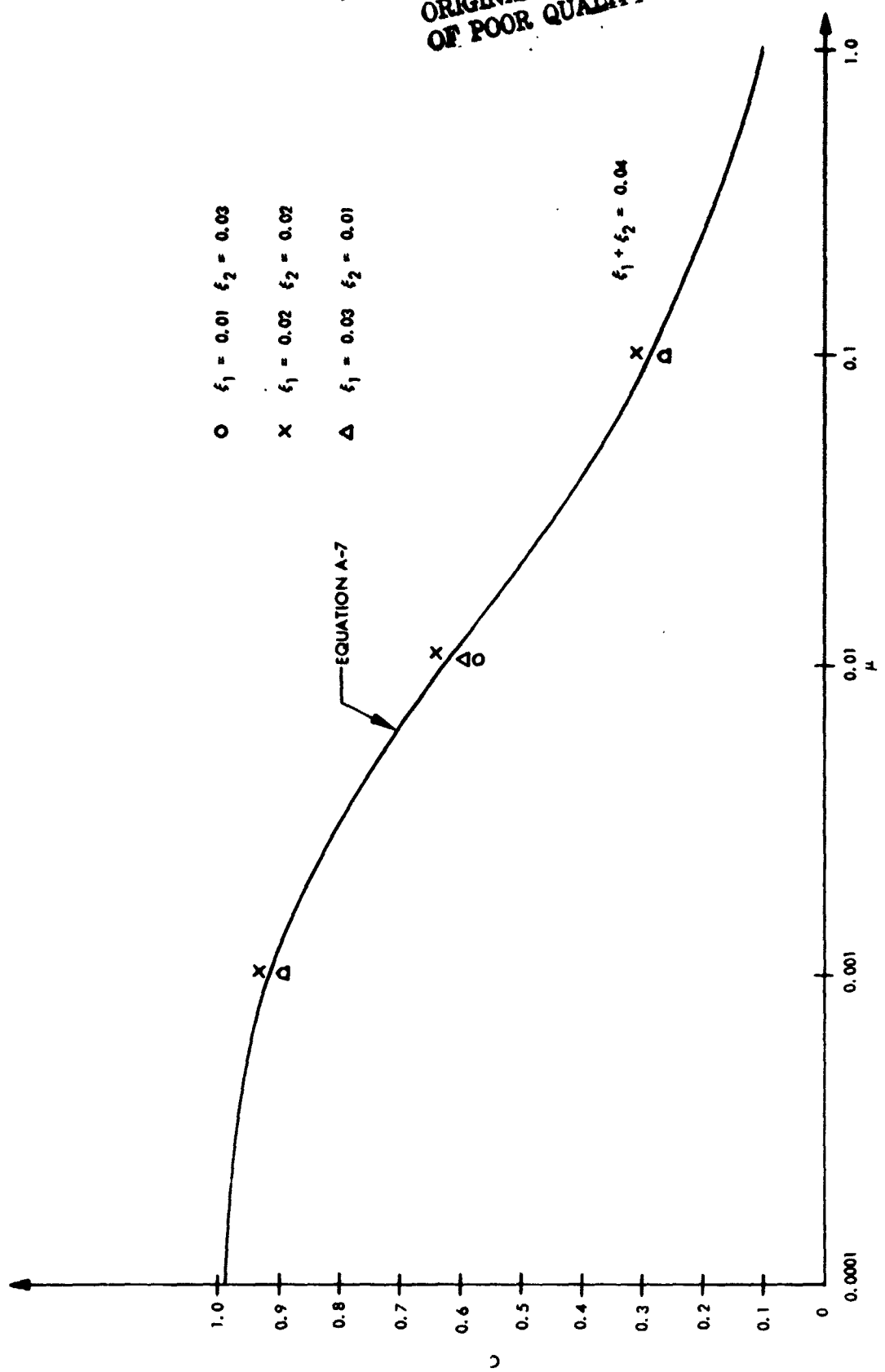


Figure A-6. Reduction Coefficient C

Table A-1. Peak Acceleration

	$\mu = 0$			$\mu = 0.001$			$\mu = 0.01$			$\mu = 0.1$			$\mu = 1.0$					
	ξ_1	ξ_2	$r = \frac{1}{p}$	0.01	0.02	0.03	0.01	0.02	0.03	0.01	0.02	0.03	0.01	0.02	0.03	0.01	0.02	0.03
0.80	3.05	3.05	3.05	3.05	3.05	3.05	2.90	2.89	2.90	2.03	2.02	2.05						
0.88	4.70	4.65	4.70	4.55	4.60	4.60	4.00	4.00	4.05	2.39	2.39	2.40						
0.92	6.00	5.94	6.06	5.80	5.75	5.85	4.80	4.78	4.81	2.51	2.52	2.52						
0.96	7.80	7.65	7.85	7.39	7.20	7.41	5.41	5.38	5.45	2.56	2.58	2.59						
0.98	8.80	8.52	8.90	8.12	7.90	8.20	5.61	5.60	5.62	2.61	2.58	2.60						
0.99	9.13	8.80	9.18	8.34	8.16	8.38	5.71	5.62	5.75	2.60	2.60	2.64						
1.00	9.43	9.00	9.35	8.55	8.35	8.45	5.80	5.75	5.78	2.60	2.61	2.60	0.935	0.938	0.945			
1.01	9.27	8.85	9.25	8.42	8.30	8.42	5.73	5.65	5.75	2.61	2.60	2.62						
1.02	9.04	8.65	9.02	8.30	8.06	8.32	5.70	5.62	5.70	2.61	2.59	2.60						
1.04	8.32	8.09	8.25	7.78	7.58	7.75	5.58	5.51	5.58	2.60	2.58	2.61						
1.08	6.82	6.67	6.80	6.57	6.44	6.54	5.15	5.17	5.15	2.55	2.53	2.54						
1.20	4.32	4.30	4.33	4.24	4.20	4.22	3.93	3.90	3.97	2.34	2.34	2.35						

ORIGINAL PAGE IS
OF POOR QUALITY

PRECEDING PAGE BLANK NOT FILMED

APPENDIX B
ANALYTICAL SOLUTION OF THE EQUATIONS OF MOTION

Analytical solution is derived here in detail for the coupled equation of motion (13):

$$\begin{bmatrix} (1 + \mu) & \mu \\ \mu & \mu \end{bmatrix} \begin{Bmatrix} \ddot{x}_1 \\ \ddot{x}_2 \end{Bmatrix} + \begin{bmatrix} 2\xi_1 \omega_1 & 0 \\ 0 & 2\xi_2 \omega_2 \mu \end{bmatrix} \begin{Bmatrix} \dot{x}_1 \\ \dot{x}_2 \end{Bmatrix} + \begin{bmatrix} \omega_1^2 & 0 \\ 0 & \omega_2^2 \mu \end{bmatrix} \begin{Bmatrix} x_1 \\ x_2 \end{Bmatrix} = \begin{Bmatrix} F_{01}(t) \\ 0 \end{Bmatrix} \quad (\text{B-1})$$

An analog solution to Equation (B-1) above has been given in Appendix A. The general solution takes a complex form, with real and imaginary parts. One approach to obtaining the analytical solution to Equation (B-1) is by first deriving and using the modal coordinates of the undamped system in Equation (B-1) to diagonalize the mass and stiffness matrices. This, however, will not diagonalize the damping matrix, but the common approximation of leaving out the off-diagonal terms will result in retaining only the real part of the solution. This is an acceptable approximation for small damping.

Let us first write the frequency equation for the damped system since properties of the damped frequency equation will be used. The form of the solution is

$$\begin{Bmatrix} x_1 \\ x_2 \end{Bmatrix} = e^{pt} \begin{Bmatrix} y_1 \\ y_2 \end{Bmatrix} \quad (\text{B-2})$$

Substituting in the left-hand side of Equation (B-1) results in the damped frequency equation:

$$\begin{aligned} \left(\frac{p}{\omega_2}\right)^4 + 2[R\xi_1 + (1 + \mu)\xi_2] \left(\frac{p}{\omega_2}\right)^3 + [R^2 + 4R\xi_1\xi_2 + (1 + \mu)] \left(\frac{p}{\omega_2}\right)^2 \\ + 2R[\xi_1 + \xi_2 R] \left(\frac{p}{\omega_2}\right) + R^2 = 0 \end{aligned} \quad (\text{B-3})$$

The undamped frequency equation is then obtained by letting $\xi_1 = \xi_2 = 0$:

$$\Omega^4 - [R^2 + (1 + \mu)] \Omega^2 + R^2 = 0 \quad (B-4)$$

where

$$\Omega = \frac{\omega}{\omega_2}$$

$$R = \frac{\omega_1}{\omega_2} = \frac{\omega_l}{\omega_s \sqrt{1 + M_{sl}}}$$

The roots to Equation (B-3) are $\omega_{n1} = \Omega_1 \omega_2$ and $\omega_{n2} = \Omega_2 \omega_2$ in which Ω_1 and Ω_2 are defined by

$$\left. \begin{aligned} \Omega_1 &= \Omega_0 - \frac{\Delta\Omega}{2} \\ \Omega_2 &= \Omega_0 + \frac{\Delta\Omega}{2} \end{aligned} \right\} (B-5)$$

and $\Omega_0 \omega_2$ and $\Delta\Omega \omega_2$, respectively, are the center and the beat frequency:

$$\left. \begin{aligned} \omega_2 \Omega_0 &= \frac{\omega_2}{2} \sqrt{(R+1)^2 + \mu} \\ \omega_2 \Delta\Omega &= \omega_2 \sqrt{(R-1)^2 + \mu} \end{aligned} \right\} (B-6)$$

Associated with the frequencies ω_{n1} and ω_{n2} obtained above are two undamped mode shapes, respectively defined by

$$\{Y_1\} = \begin{Bmatrix} \frac{1}{\Omega_1^2} - 1 \\ \hline 1 \end{Bmatrix} \quad \text{and} \quad \{Y_2\} = \begin{Bmatrix} \frac{1}{\Omega_2^2} - 1 \\ \hline 1 \end{Bmatrix} \quad (\text{B-7})$$

Next, the classical coordinate transformation is applied to x_1 and x_2 to diagonalize the matrices of Equation (B-1):

$$\begin{Bmatrix} x_1 \\ x_2 \end{Bmatrix} = [Y_1 | Y_2] \begin{Bmatrix} z_1 \\ z_2 \end{Bmatrix} \quad (\text{B-8})$$

This results in:

$$\begin{Bmatrix} \ddot{z}_1 \\ \ddot{z}_2 \end{Bmatrix} + 2\omega_2 \begin{Bmatrix} \frac{1}{\lambda_1} \left[\xi_1 R \frac{(1 - \Omega_1^2)^2}{\Omega_1^4} + \xi_2 \mu \right] \\ \hline \frac{1}{\lambda_2} \left[\frac{\mu}{R} (R\xi_2 - \xi_1) \right] \\ \hline \frac{1}{\lambda_2} \left[\frac{\mu}{R} (R\xi_2 - \xi_1) \right] \\ \hline \frac{1}{\lambda_1} \left[\xi_1 R \frac{(1 - \Omega_2^2)^2}{\Omega_2^4} + \xi_2 \mu \right] \end{Bmatrix} \begin{Bmatrix} \dot{z}_1 \\ \dot{z}_2 \end{Bmatrix} + \begin{Bmatrix} \omega_{n1}^2 & 0 \\ 0 & \omega_{n2}^2 \end{Bmatrix} \begin{Bmatrix} z_1 \\ z_2 \end{Bmatrix} = \begin{Bmatrix} \frac{1}{\lambda_1} \left(\frac{1}{\Omega_1^2} - 1 \right) \\ \frac{1}{\lambda_2} \left(\frac{1}{\Omega_2^2} - 1 \right) \end{Bmatrix} F_0(t) \quad (\text{B-9})$$

where

$$\lambda_1 = \frac{1}{\Omega_1^4} [(1 - \Omega_1^2)^2 + \mu]$$

$$\lambda_2 = \frac{1}{\Omega_2^4} [(1 - \Omega_2^2)^2 + \mu]$$

are the generalized mass.

ORIGINAL PAGE IS
OF POOR QUALITY

It is seen that the off-diagonal terms in the damping matrix will vanish when the damping ratio is proportional to the frequency ratio. No such limitation will be imposed, and therefore, $\xi_1/\xi_2 \neq \omega_1/\omega_2$. However, the magnitude of the off-diagonal terms will be assumed small enough to be neglected in subsequent calculations. This is equivalent to neglecting the imaginary part of the solution, a commonly used approximation that results in decoupling Equation (B-9), so that

$$\left. \begin{aligned} \ddot{z}_1 + 2\xi_{n1}\omega_{n1}\dot{z}_1 + \omega_{n1}^2 z_1 &= \frac{1 - \Omega_1^2}{\Omega_1^2 \lambda_1} F_{0l}(t) \\ \ddot{z}_2 + 2\xi_{n2}\omega_{n2}\dot{z}_2 + \omega_{n2}^2 z_2 &= \frac{1 - \Omega_2^2}{\Omega_2^2 \lambda_2} F_{0l}(t) \end{aligned} \right\} \text{(B-10)}$$

where now:

$$2\omega_{n1}\xi_{n1} = \frac{2\omega_2}{\lambda_1} \left[\xi_1 R \frac{(1 - \Omega_1^2)^2}{\Omega_1^4} + \xi_2 \mu \right]$$

$$2\omega_{n2}\xi_{n2} = \frac{2\omega_2}{\lambda_2} \left[\xi_1 R \frac{(1 - \Omega_2^2)^2}{\Omega_2^4} + \xi_2 \mu \right]$$

Furthermore, from the theory of equation, the sum of the roots of the damped frequency equation, Equation (B-3), is equal to the coefficient of $(p/\omega_2)^3$. Therefore:

$$\xi_{n1}\omega_{n1} + \xi_{n2}\omega_{n2} = 2\beta\omega_2 \quad \text{(B-11)}$$

where

$$\beta = \frac{1}{2} [\xi_1 R + (1 + \mu) \xi_2]$$

The following approximate relationship will be useful:

$$\xi_{n1} \omega_{n1} - \xi_{n2} \omega_{n2} = 2\theta \omega_2 \quad (\text{B-12})$$

where

$$\theta = \frac{1}{\lambda_1} \left[\xi_1 R \left(\frac{1}{\Omega_1^2} - 1 \right)^2 + \xi_2 \mu \right] - \frac{1}{2} \left[\xi_1 R + (1 + \mu) \xi_2 \right]$$

Equations (B-10) may now be solved for a prescribed force system $F_{O\ell}(t)$. The specific case when $F_{O\ell}(t)$ is an impulse delta function of amplitude $F_{O\ell}$ applied at $t = 0$ is discussed. By definition, the impulse $F_{O\ell}(t) = F_{O\ell} \delta(t)$ is the response of an initial velocity $v_{O\ell}$. Numerically $F_{O\ell} = v_{O\ell}$ for an impulse applied to a unit mass, as it is the case for Equation (B-9). The homogeneous solution of Equation (B-10) is:

$$Z_r = A_r e^{-\xi_{nr} \omega_{nr} t} \sin \bar{\omega}_{nr} t + B_r e^{-\xi_{nr} \omega_{nr} t} \cos \bar{\omega}_{nr} t \quad (\text{B-13})$$

where $\bar{\omega}_{nr} = \omega_{nr} \sqrt{1 - \xi_{nr}^2}$ = damped natural frequency and A_r, B_r are constants ($r = 1$ for launch vehicle; $r = 2$ for the spacecraft).

The initial conditions for the system at $t = 0$ are

$$x_1(0) = x_2(0) = 0$$

$$\dot{x}_1(0) = v_{O\ell} \quad \text{and} \quad \dot{x}_2(0) = 0 \quad (\text{B-14})$$

By combining the transformation of (B-8) with the general solution of (B-13) and the initial conditions in (B-14), we have

ORIGINAL PAGE IS
OF POOR QUALITY

$$\begin{aligned}
 x_1(t) &= \frac{v_{0l}}{(\Omega_2^2 - \Omega_1^2)} \left[\frac{\Omega_2^2(1 - \Omega_1^2)}{\bar{\omega}_{n1}} e^{-\xi_{n1}\omega_{n1}t} \sin \bar{\omega}_{n1}t \right. \\
 &\quad \left. - \frac{\Omega_1^2(1 - \Omega_2^2)}{\bar{\omega}_{n2}} e^{-\xi_{n2}\omega_{n2}t} \sin \bar{\omega}_{n2}t \right] \\
 x_2(t) &= \frac{R^2 v_{0l}}{(\Omega_2^2 - \Omega_1^2)} \left[\frac{1}{\bar{\omega}_{n1}} e^{-\xi_{n1}\omega_{n1}t} \sin \bar{\omega}_{n1}t \right. \\
 &\quad \left. - \frac{1}{\bar{\omega}_{n2}} e^{-\xi_{n2}\omega_{n2}t} \sin \bar{\omega}_{n2}t \right]
 \end{aligned}
 \tag{B-15}$$

PRECEDING PAGE BLANK NOT FILMED

APPENDIX C

RECOVERY OF LAUNCH VEHICLE MODAL PROPERTIES

A. EQUATIONS OF MOTION

In this appendix, equations are derived whereby the modes and modal responses of the launch vehicle with an interface loaded by only a rigid mass can be recovered from the given modes and modal responses of the same launch vehicle whose interface is loaded by an elastic and a rigid-mass simulation of the spacecraft. Let the subscripts S denote cantilevered spacecraft modes, and the subscripts C denote the composite launch vehicle free-free modes with an elastically loaded interface, see Figure C-1. The motion of the total composite system of spacecraft and launch vehicle in Figure C-1 subjected to an external force $\{F_j\}$ is governed by the set of equations:

$$\{\ddot{q}_c\} + [2\xi_c \omega_c] \{\dot{q}_c\} + [\omega_c^2] \{q_c\} = [\phi_{cj}] \{F_j\} \quad (C-1)$$

where \ddot{q}_c are available from the launch vehicle analysis.

The modes of the launch vehicle with a rigid-mass can be computed from Equation (C-1) by subtracting the modal reactions of the elastic spacecraft at the interface. This is analogous to Equation (2) of the main text in which the sign of the spacecraft reaction force $\{F_i\}$ is negative since the spacecraft that was originally put on the launch vehicle is now being removed. In this case, the generalized coordinates are denoted by $\{q'_c\}$ instead of $\{q_c\}$:

$$\{\ddot{q}'_c\} + [2\xi_c \omega_c] \{\dot{q}'_c\} + [\omega_c^2] \{q'_c\} = [\phi_{cj}] \{F_j\} - [\phi_{ci}] \{-F_i\} \quad (C-2)$$

From Equations (8) and (4):

$$\left. \begin{aligned} \{F_i\} &= [M_{ii}] \{\ddot{R}_i\} + [m_{is}] \{\ddot{q}'_s\} \\ \{\ddot{R}_i\} &= [\phi_{.i}] \{\ddot{q}'_c\} \\ [M_{ii}] &= [M_{ii}]_{RES} + \sum_{s=1}^S [m_{ii}^s] \end{aligned} \right\} \quad (C-3)$$

ORIGINAL PAGE IS
OF POOR QUALITY

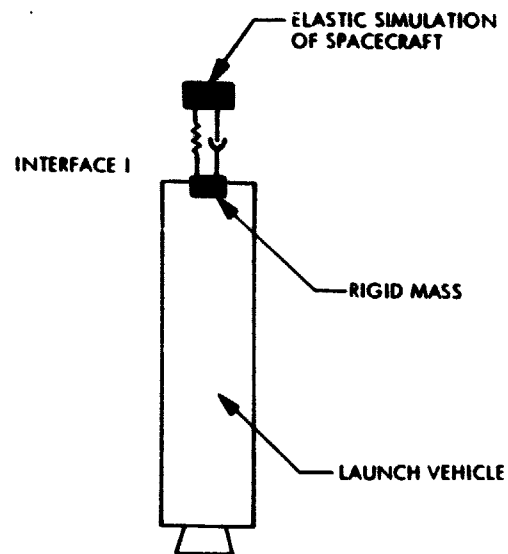


Figure C-1. Composite Launch Vehicle With Elastically Loaded Interface

Also, from Equation (3) of the main text, the spacecraft is governed by:

$$\{\ddot{q}'_s\} + [2\xi_s \omega_s] \{\dot{q}'_s\} + [\omega_s^2] \{q'_s\} = -[m_{si}] \{\ddot{R}'_i\} \quad (C-4)$$

Equations (C-2, C-3, and C-4) are now combined to give the governing equations for the rigid-mass-loaded launch vehicle response:

$$\left[\begin{array}{c|c} ([I] - [\phi_{ci}][M_{ii}][\phi_{ic}]) & -[\phi_{ci}][m_{is}] \\ \hline -[m_{si}][\phi_{ic}] & -[I] \end{array} \right] \begin{Bmatrix} \ddot{q}'_c \\ \ddot{q}'_s \end{Bmatrix} + \left[\begin{array}{c|c} 2\xi_c \omega_c & 0 \\ \hline 0 & -2\xi_s \omega_s \end{array} \right] \begin{Bmatrix} \dot{q}'_c \\ \dot{q}'_s \end{Bmatrix} + \left[\begin{array}{c|c} \omega_c^2 & 0 \\ \hline 0 & -\omega_s^2 \end{array} \right] \begin{Bmatrix} q'_c \\ q'_s \end{Bmatrix} = \begin{Bmatrix} [\phi_{cj}]\{F_j\} \\ 0 \end{Bmatrix} \quad (C-5)$$

In a concise form, Equation (C-5) is written as:

$$[\tilde{M}]\{\ddot{q}'\} + [\tilde{D}]\{\dot{q}'\} + [\tilde{\omega}^2] \{q'\} = \{F\}$$

and its undamped homogeneous part is written as

$$[\tilde{M}]\{\ddot{q}'\} + [\tilde{\omega}^2] \{q'\} = 0 \quad (C-6)$$

B. EIGENVALUE SOLUTION

In general, if the system of composite modes, C, contained S-spacecraft elastic modes, and L-launch vehicle rigid-and-elastic modes $C = S + L$, the undamped eigenvalue solution of Equation (C-6) will result in $(L + 2S)$ eigenvalues $\Omega_L, \Omega_{s1}, \Omega_{s2}$ and associated eigenvectors $\{V_L\}, \{V_{s1}\}, \{V_{s2}\}$.

Of these, two S-roots will be repeated, $\Omega_{s1} = \Omega_{s2}$, and are associated with the elastic modes of the spacecraft. The remaining L-roots are associated with the rigid-mass-loaded launch vehicle free-free modes,

**ORIGINAL PAGE IS
OF POOR QUALITY**

some of which will correspond to rigid body modes with zero frequencies, and the remaining modes will correspond to elastic modes with nonzero frequencies. The $(L + 2S)$ set of modes collectively referred to as $\{V\}$

$$\{V\} = [v_L \mid v_{s1} \mid v_{s2}] \quad (C-7)$$

will transform Equation (C-6) to the diagonal form

$$\{I\}\{\ddot{Q}\} + [\Omega^2]\{Q\} = 0 \quad (C-8)$$

with

$$\{q'\} = \{V\}\{Q\} \quad (C-9)$$

C. MODE SHAPES AND ACCELERATIONS AT THE INTERFACE

The acceleration $\{\ddot{R}_i\}$ at the interface can be expressed in either the $\{q'\}$ or $\{Q\}$ coordinates. Thus,

$$\{\ddot{R}_i\} = [\phi_i]\{\ddot{q}'\} \quad (C-10)$$

or

$$\{\ddot{R}_i\} = [\psi_i]\{\ddot{Q}\}$$

where $[\phi_i]$ and $[\psi_i]$ are the mode shapes at the interface in the $\{q'\}$ and the $\{Q\}$ coordinates, respectively.

Because of Equation (C-9),

$$\begin{aligned} \{\ddot{R}_i\} &= [\phi_i]\{\ddot{q}'\} = [\phi_i][V]\{\ddot{Q}\} \\ &= [\psi_i]\{\ddot{Q}\} \end{aligned}$$

then

$$[\psi_i] = [\phi_i][V] \quad (C-11)$$

D. MODAL ACCELERATION TIME HISTORY ($\ddot{Q}(t)$)

The time history of the modal acceleration corresponding to the newly obtained rigid-mass-loaded launch vehicle modes $\{Q\}$ are obtained from Equation (C-9) so that

$$\{\ddot{Q}\} = [V^{-1}]\{\ddot{q}'\} \quad (C-12)$$

The inverse $[V^{-1}]$ in Equation (C-12) need not be performed. It can be found from the orthogonality condition that led to Equation (C-8):

$$[V^T][\tilde{M}][V] = [I]$$

so that

$$[V^{-1}] = [V^T][\tilde{M}] \quad (C-13)$$

Therefore,

$$\{\ddot{Q}\} = [V^T][\tilde{M}]\{\ddot{q}'\} \quad (C-14)$$

However, $\{\ddot{q}\}$ rather than $\{\ddot{q}'\}$ are usually available from the launch vehicle analysis. Computing $\{\ddot{q}'\}$ as a transient solution of Equation (C-5) is straightforward, but is both costly and unnecessary. For this reason, two approximate alternative solutions are shown next that give very acceptable accuracy at low cost.

1. Approximate Solution 1

Since the right-hand sides of Equations (C-1) and (C-5) are identical, they may be combined to yield the following exact expression:

$$[\tilde{M}] \begin{Bmatrix} \ddot{q}'_c \\ \ddot{q}'_s \end{Bmatrix} = \begin{Bmatrix} \ddot{q}_c \\ \frac{[\omega_s^2]\{q'_s\} + [2\xi_s \omega_s]\{\dot{q}'_s\}}{\ddot{q}_c} \end{Bmatrix} + [2\xi_c \omega_c]\{\dot{q}_c - \dot{q}'_c\} + [\omega_c^2]\{q_c - q'_c\} \quad (C-15)$$

ORIGINAL PAGE IS
OF POOR QUALITY

For the rigid body modes $\omega_c = 0$, the last two terms of Equation (C-15) are identically zero. However, for the elastic modes, these last two terms are small because they express differences between two quantities of global character having little dependence on the presence of the relatively small spacecraft. On account of this reasoning, the last two terms of Equation (C-15) can be neglected with little loss in accuracy. This implies:

$$q_c \doteq q'_c \quad \text{and} \quad \dot{q}_c \doteq \dot{q}'_c \tag{C-16}$$

Also,

$$q_s \doteq q'_s \quad \text{and} \quad \dot{q}_s \doteq \dot{q}'_s$$

Now, Equation (C-15) is approximately written as

$$[\bar{M}] \begin{Bmatrix} \ddot{q}'_c \\ \ddot{q}'_s \end{Bmatrix} \doteq \begin{Bmatrix} \ddot{q}_c \\ \frac{\ddot{q}_c}{[\omega_s^2]\{q'_s\} + [2\xi_s \omega_s]\{\dot{q}'_s\}} \end{Bmatrix} \tag{C-17}$$

which, when solved with Equation (C-14), yields

$$\{\ddot{q}\} \doteq [V^T] \begin{Bmatrix} \ddot{q}_c \\ \frac{\ddot{q}_c}{[\omega_s^2]\{q'_s\} + [2\xi_s \omega_s]\{\dot{q}'_s\}} \end{Bmatrix} \tag{C-18}$$

The modal coordinates $\{q'_s\}$ and $\{\dot{q}'_s\}$ of the elastic simulation of the spacecraft may be obtained from an inexpensive transient solution since they are usually small (of the order of 3 to 6 modes). In this case, the lower partition of Equation (C-5) can be solved for $\{q'_s\}$ and $\{\dot{q}'_s\}$ approximately by replacing $\{\ddot{q}'_c\}$ by $\{\ddot{q}_c\}$:

$$\{\ddot{q}'_s\} + [2\xi_s \omega_s]\{\dot{q}'_s\} + [\omega_s^2]\{q'_s\} \doteq -[m_{si}][\phi_{ic}]\{\ddot{q}_c(t)\} \tag{C-19}$$

The approximation above is acceptable because $\{\ddot{q}_s'\}$ is affected only to the second order by $\{\ddot{q}_c\}$ or $\{\ddot{q}_c'\}$, and also because there is no tuning between ω_s and ω_c since ω_c never contains ω_s exactly.

Thus, Equation (C-18) is alternatively expressed as:

$$\{\ddot{q}\} \doteq [V^T] \left\{ \begin{array}{c} \ddot{q}_c \\ \hline -\{\ddot{q}_s'\} - [m_{si}][\phi_{ic}]\{\ddot{q}_c\} \end{array} \right\} \quad (C-20)$$

2. Approximate Solution 2

Let the subscripts cR and cE, respectively, denote the subset of rigid body modes and the subset of elastic modes constituting the total number of the composite modes c. Thus $c = cR + cE$. This second approximation is based on the premise that, except for the rigid body modal accelerations $\{\ddot{q}_{cR}\}$ and $\{\ddot{q}_{cR}'\}$, the acceleration time history of all the elastic composite modes are negligibly affected by the presence of the elastic simulation of the spacecraft. Therefore, for the elastic composite modes:

$$\{\ddot{q}_{cE}'(t)\} \doteq \{\ddot{q}_{cE}(t)\} \quad (C-21)$$

However, for the rigid body modes, Equation (C-1) gives

$$\{\ddot{q}_{cR}\} = [\phi_{cRj}]\{F_j\} \quad (C-22)$$

Also, Equation (C-2) for the rigid-mass-loaded launch vehicle gives

$$\{\ddot{q}_{cR}'\} = [\phi_{cRj}]\{F_j\} + [\phi_{cRi}]\{F_i\} \quad (C-23)$$

ORIGINAL PAGE IS
OF POOR QUALITY

Solving Equations (C-22) and (C-23), and making use of (C-3), we get

$$\begin{aligned} \left([I] - [\phi_{cRi}][M_{ii}][\phi_{icR}] \right) \{\ddot{q}_{cR}'\} &= \{\ddot{q}_{cR}\} + [\phi_{cRi}][m_{is}]\{\ddot{q}_s\} \\ &+ [\phi_{cRi}][M_{ii}][\phi_{icE}]\{\ddot{q}_{cE}\} \quad (C-24) \end{aligned}$$

In the approximation of Equation (C-24), $\{\ddot{q}_s\}$ is computed in the same manner from Equation (C-19) of the previous approximation. As such, Equations (C-21) and (C-24) along with Equation (C-19) provide an approximate alternative to computing all members of $\{\ddot{q}'\}$. Then again, Equation (C-14) is used to compute $\{\ddot{Q}\}$.

PRECEDING PAGE BLANK NOT FILMED

ORIGINAL PAGE IS
OF POOR QUALITY

APPENDIX D

DISPLACEMENT SPECTRA FOR THE GENERALIZED
RIGID BODY MODES

In this appendix, an expression is derived for the generalized modal displacement spectra, Q_{sl} , that should be used for the rigid body modes ($R = 0$) in place of Equation (23) of the main text.

From the lower partition of Equation (13),

$$\ddot{x}_2 + 2\xi_2\omega_2\dot{x}_2 + \omega_2^2x_2 = -\ddot{x}_1 \quad (D-1)$$

where, according to Equation (14),

$$\ddot{x}_1 = (1 + M_{sl}) \ddot{q}_k \quad (D-2)$$

The homogeneous solution of Equation (D-1) having initial conditions $x_2(0) = x_0$ and $\dot{x}_2(0) = \dot{x}_0$ is:

$$x_2^h(t) = e^{-\xi_2\omega_2 t} \left[\frac{1}{\bar{\omega}_2} (\dot{x}_0 + \xi_2\omega_2 x_0) \sin \bar{\omega}_2 t + x_0 \cos \bar{\omega}_2 t \right] \quad (D-3)$$

The particular solution of Equation (D-1) is:

$$x_2^p(t) = \frac{1}{\bar{\omega}_2} \int_{\bar{t}=0}^{\bar{t}=t} \ddot{x}_1(\bar{t}) e^{-\xi_2\omega_2(t-\bar{t})} \sin \bar{\omega}_2(t-\bar{t}) d\bar{t} \quad (D-4)$$

where

$$\bar{\omega}_2 = \omega_2 \sqrt{1 - \xi_2^2}$$

Thus, the total solution of Equation (D-1) is

$$x_2(t) = x_2^h + x_2^p \quad (D-5)$$

Now, the spacecraft modal response $q_s(t)$ to rigid body launch vehicle input ($R = 0$) is given by

$$q_s(t) = \frac{\sqrt{m_{sl}}}{1 + M_{sl}} x_2(t) \quad (D-6)$$

ORIGINAL PAGE IS
OF POOR QUALITY

and the generalized modal displacement Q_{sl} for such cases is given by the maximum of Equation (D-6). Therefore,

$$Q_{sl} = \frac{\sqrt{m_{sl}}}{1 + M_{sl}} \left| x_2(t) \right|_{\max} \quad (D-7)$$

Where again, $R = 0$ and $x_2(t)$ are defined by Equations (D-3) through (D-5).

The homogeneous solution $x_2^h(t)$ can be ignored by starting to compute the forcing function well before the actual event, and only Equation (D-4) needs to be considered. Then Equation (D-7) becomes

$$Q_{sl} = \frac{\sqrt{m_{sl}}}{1 + M_{sl}} \left| x_2^p(t) \right|_{\max}$$

Furthermore, by definition, $\left| x_2^p(t) \right|_{\max}$ is the relative displacement shock spectra of $\ddot{x}_1(t) = (1 + M_{sl}) \ddot{q}_l(t)$

$$\left| x_2^p(t) \right|_{\max} = D_e^p (1 + M_{sl}) = \frac{A_l^p}{\omega_2} (1 + M_{sl})$$

where A_l^p is the acceleration shock spectra. Then

$$Q_{sl} = \sqrt{m_{sl}} \frac{A_l^p}{\omega_2} \quad l = 1, 2, \dots, 6$$

This is the same limit that Equation (23) takes for $R \rightarrow 0$. Thus,

$$(\omega_l v_{0l})_{R \rightarrow 0} = A_l^p \quad (D-8)$$

where $\omega_l = \omega_1$.